# Chapter 4
# Results

## 4.1. Phytochemical analysis

### 4.1.1. Qualitative phytochemical screening

The results of qualitative screening of various classes of phytochemicals are enlisted in Table 1.

**Table 1:** Qualitative determination of various classes of phytochemicals present in leaf of *C. bonplandianus.*

| Phytochemicals | Leaf |
|---|---|
| Tannin | + |
| Phlobatannin | + |
| Cholesterol | + |
| Terpinoid | + |
| Glycoside | + |
| Phenolics | + |
| Flavonoid | + |
| Steroid | + |
| Anthraquinone | - |
| Saponin | + |
| Carbohydrate | + |
| Protein | + |
| Alkaloid | + |

### 4.1.2. Quantitative phytochemical screening

The results of quantitative screening of various classes of phytochemicals are enlisted in Table 2.

### 4.1.3. Gas chromatography-mass spectrometry (GC-MS) analysis

GC-MS analysis showed the chemical fingerprint of the CBL extract (Figure 8 and Table 3). The GC-MS data reported that the presences of several bioactive compounds, of which many of them are documented, possess distinct and definitive pharmacological activities.

### 4.1.4. Fourier transforms infrared spectroscopy (FTIR) analysis

FTIR analysis of CBLE (Figure 68-70) was performed to identify the predominant chemical groups present in the extracts. Peak shifts in FTIR analysis are very common phenomenon. Some of the functional groups may thus, be affected by peak shift. The IR spectrum (Figure 9) of CBLE displayed different peaks (Table 4) at corresponding to different functional groups (Silverstein *et al.,* 2007).

**Table 2:** Quantitative determination of various phytochemicals present in leaf of *C. bonplandianus.* All values are represented as mean ± SD of three replicative assays.

| Phytochemicals | Mean | S.D. | S.E.M. | Variance | Coef. Var. |
|---|---|---|---|---|---|
| **Flavonoid**[e] | 4.36 | 0.48 | 0.27 | 0.23 | 0.11 |
| **Alkaloid**[d] | 59.60 | 4.79 | 2.76 | 23.00 | 0.08 |
| **Saponin**[d] | 17.19 | 1.35 | 0.78 | 1.82 | 0.07 |
| **Phenol**[e] | 75.29 | 3.19 | 1.84 | 10.21 | 0.04 |
| **Ascorbic acid**[f] | 0.71 | 0.05 | 0.02 | 0.00 | 0.07 |
| **Thiamine**[f] | 0.54 | 0.01 | 0.00 | 0.00 | 0.02 |
| **Riboflavin**[f] | 0.55 | 0.03 | 0.01 | 0.00 | 0.05 |
| **Total protein**[e] | 55.04 | 2.09 | 1.20 | 4.38 | 0.03 |
| **Lipid**[e] | 37.53 | 2.46 | 1.42 | 6.09 | 0.06 |
| **Soluble sugar**[e] | 2.53 | 0.40 | 0.23 | 0.16 | 0.15 |
| **Tannin**[f] | 26.18 | 2.63 | 1.52 | 6.95 | 0.10 |
| **Moisture**[g] | 65.20 | 3.19 | 1.84 | 10.18 | 0.04 |
| **Ash**[g] | 1.53 | 0.24 | 0.13 | 0.05 | 0.15 |

S.D. = Standard deviation; SEM=Standard error of mean; Coef.Vr=Co-efficient of Variance. All values are the mean of three replicate experiments. d Units are in g/100g; e Units are in mg/g; f Units are in mg/100g; g Units are in %.

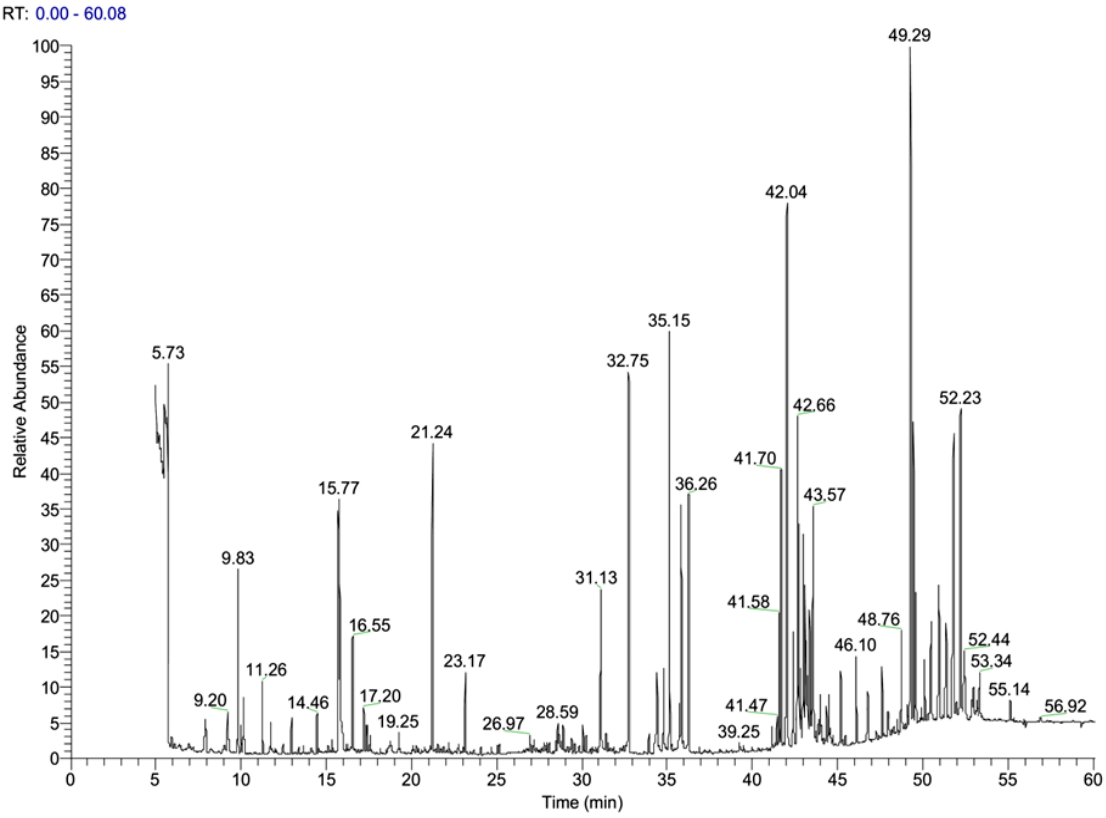


**Figure 8:** Gas Chromatography Mass Spectrometry (GC-MS) analysis of *Croton bonplandianus*.

**Table 3:** Chemical fingerprint of CBL extract revealed by GC-MS analyses corresponding to Figure 8.

| Compounds name | Molecular weight | Formula | RT |
|---|---|---|---|
| 2-Pyrrolidinone, 1-methyl- | 99 | C5H9NO | 9.20 |
| Propanoic acid, 2-[(trimethylsilyl)oxy]-, trimethylsilyl ester | 234 | C9H22O3Si2 | 9.83 |
| Hexanoic acid, trimethylsilyl ester | 188 | C9H20O2Si | 10.01 |
| 2-Methyl-4-pentenoic acid, trimethylsilyl ester | 186 | C9H18O2Si | 10.14 |
| Acetic acid, [(trimethylsilyl)oxy]-, trimethylsilyl ester | 220 | C8H20O3Si2 | 10.19 |
| 2-Hexenoic acid, trimethylsilyl ester | 185 | C9H18O2Si | 11.26 |
| Ethanedioic acid, bis(trimethylsilyl) ester(syn. Oxalic acid, bis (trimethylsilyl) ester) | 234 | C8H18O4Si2 | 11.72 |
| Propanoic acid, 3-[(trimethylsilyl)oxy]-, trimethylsilyl ester | 234 | C9H22O3Si2 | 12.01 |
| p-Trimethylsiloxybenzaldehydeoxime, trimethylsilyl- | 281 | C13H23NO2Si2 | 12.09 |
| Butanoic acid, 3-[(trimethylsilyl)oxy]-, trimethylsilyl ester(syn. β-Hydroxybutyric acid (2TMS)) | 248 | C10H24O3Si2 | 12.47 |
| Propanedioic acid, bis(trimethylsilyl) ester | 248 | C9H20O4Si2 | 13.66 |
| D-Erythro-Pentonic acid, 2-deoxy-3,5-bis-O-(trimethylsilyl)-, γ-lactone | 276 | C11H24O4Si2 | 14.13 |
| 1,3-Bis(trimethylsilyloxy)butane | 234 | C10H26O2Si2 | 14.46 |
| 1-Phenylethanol, tert-butyldimethylsilyl ether | 236 | C14H24OSi | 14.63 |
| Octanoic acid, trimethylsilyl ester | 216 | C11H24O2Si | 15.11 |
| Glycerol, tris(trimethylsilyl) ether | 308 | C12H32O3Si3 | 15.70 |
| Phosphoric acid, tris(trimethylsilyl) ester | 314 | C9H27O4PSi3 | 15.77 |
| Butane, 1,2,3-tris(trimethylsiloxy)- | 322 | C13H34O3Si3 | 16.19 |
| Butanedioic acid, bis(trimethylsilyl) ester | 262 | C10H22O4Si2 | 16.55 |
| Glyceric acid, (3TMS) | 322 | C12H30O4Si3 | 17.20 |
| Itaconic acid, bis-TMS ester | 274 | C11H22O4Si2 | 17.35 |
| Fumaric acid, bis(trimethylsilyl) ester | 260 | C10H20O4Si2 | 17.40 |
| Methylmaleic acid, bis(trimethylsilyl) ester | 274 | C11H22O4Si2 | 17.57 |
| 2(3H)-Furanone, dihydro-3,4-bis[(trimethylsilyl)oxy]-, trans- | 262 | C10H22O4Si2 | 18.19 |
| Methylmaleic acid, bis(trimethylsilyl) ester | 274 | C11H22O4Si2 | 18.78 |
| β-Caryophyllen | 204 | C15H24 | 19.25 |
| Decanoic acid, trimethylsilyl ester | 244 | C13H28O2Si | 20.11 |
| Butanedioic acid, [(trimethylsilyl)oxy]-, bis(trimethylsilyl) ester (syn. Malic acid (3TMS) | 350 | C13H30O5Si3 | 21.24 |
| L-Threonic acid, tris(trimethylsilyl) ether, trimethylsilyl ester | 424 | C16H40O5Si4 | 23.17 |
| Pentanedioic acid, 2-[(trimethylsilyl)oxy]-, bis(trimethylsilyl) ester (syn. 2-Hydroxyglutaric acid, tri-TMS) | 364 | C14H32O5Si3 | 23.26 |
| Ethanol, 2-(octadecyloxy)-(syn. 2-Octadecyloxyethanol) | 314 | C20H42O2 | 23.44 |
| Dodecanoic acid, trimethylsilyl ester | 272 | C15H32O2Si | 24.71 |
| Ribitol, 1,2,3,4,5-pentakis-O-(trimethylsilyl)- | 512 | C20H52O5Si5 | 25.17 |
| 14-Methyl-pentadecane-1,2-diol, bis(trimethylsilyl) ether | 402 | C22H50O2Si2 | 26.57 |
| Benzoic acid, 2-[(trimethylsilyl)oxy]-, trimethylsilyl ester(syn. Benzoic acid, 2-[(trimethylsilyl)oxy]-, trimethylsilyl ester) | 282 | C13H22O3Si2 | 26.76 |
| 5,8,11-Eicosatriynoic acid, trimethylsilyl ester | 372 | C23H36O2Si | 26.97 |
| Ethanol, (2-(3,4-dihydroxyphenyl)-, tris(trimethylsilyl)- | 370 | C17H34O3Si3 | 27.43 |

*Contd… to next page.*

*Contd… from previous page.*

| Compounds name | Molecular weight | Formula | RT |
|---|---|---|---|
| Cinnamic acid, p-(trimethylsiloxy)-, trimethylsilyl ester (syn. p-Coumaric acid, bis-TMS) | 308 | C15H24O3Si2 | 27.79 |
| Tetradecanoic acid, trimethylsilyl ester | 300 | C17H36O2Si | 28.90 |
| D-Pinitol, pentakis(trimethylsilyl) ether | 554 | C22H54O6Si5 | 29.87 |
| 1,5-Anhydro-D-sorbitol, tetrakis(trimethylsilyl) ether | 452 | C18H44O5Si4 | 30.06 |
| n-Hexadecanoic acid (syn. Palmitic acid) | 256 | C16H32O2 | 31.13 |
| L-Ascorbic acid, 2,3,5,6-tetrakis-O-(trimethylsilyl)-(syn. Ascorbic acid (4TMS) | 464 | C18H40O6Si4 | 31.42 |
| Hexadecanoic acid, trimethylsilyl ester | 328 | C19H40O2Si | 32.75 |
| Phytol | 296 | C20H40O | 33.95 |
| 9,12-Octadecadienoic acid (Z,Z)-(syn. Linoleic acid) | 280 | C18H32O2 | 34.28 |
| 9,12,15-Octadecatrienoic acid, (Z,Z,Z)- | 278 | C18H30O2 | 34.41 |
| Octadecanoic acid (stn. Stearic acid,) | 284 | C18H36O2 | 34.81 |
| Ethyl iso-allocholate | 436 | C26H44O5 | 35.28 |
| α-Linolenic acid, trimethylsilyl ester | 350 | C21H38O2Si | 35.83 |
| Octadecanoic acid, trimethylsilyl ester (syn. Stearic acid, trimethylsilyl ester) | 356 | C21H44O2Si | 36.26 |
| Eicosanoic acid, trimethylsilyl ester (syn. Arachidic acid, trimethylsilyl ester) | 384 | C23H48O2Si | 29.50 |
| psi.,.psi.-Carotene, 1,1',2,2'-tetrahydro-1,1'-dimethoxy- | 600 | C42H64O2 | 40.00 |
| Sucrose, octakis(trimethylsilyl) ether | 918 | C36H86O11Si8 | 41.70 |
| D-(+)-Turanose, octakis(trimethylsilyl) ether | 918 | C36H86O11Si8 | 42.04 |
| α-D-Glucopyranoside, 1,3,4,6-tetrakis-O-(trimethylsilyl)-β-D-fructofuranosyl 2,3,4,6-tetrakis-O-(trimethylsilyl)- | 918 | C36H86O11Si8 | 42.66 |
| 1-Monolinoleoylglycerol trimethylsilyl ether | 498 | C27H54O4Si2 | 44.49 |
| Squalene | 410 | C30H50 | 45.20 |
| Hentriacontane | 436 | C31H64 | 46.10 |
| Tocopherol-γ-tms-derivative | 488 | C31H56O2Si | 47.62 |
| 1-Octacosanol, trimethylsilyl ether | 482 | C31H66OSi | 49.29 |
| (+)-α-Tocopherol, O-trimethylsilyl- | 502 | C32H58O2Si | 49.46 |
| 17-Pentatriacontene | 490 | C35H70 | 50.11 |
| Campesterol, TMS ether | 472 | C31H56OSi | 50.95 |
| Stigmasterol trimethylsilyl ether | 484 | C32H56OSi | 51.38 |
| β-Sitosteroltrimethylsilyl ether | 586 | C32H58OSi | 52.23 |
| α-Amyrin, trimethylsilyl ether | 498 | C33H58OSi | 52.98 |

**Table 4:** Fourier transform infrared spectroscopy peak values of *C. bonplandianus*.

| Characteristic Absorptions (cm-1) | Type of bonds | Functional Group | Type of Vibration | Intensity |
|---|---|---|---|---|
| **3691.63** | | | | |
| **3691.28** | | | | |
| **3691.58** | | | | |
| **3677.85** | | | | |
| **3677.88** | | | | |
| **3651.33** | | | | |
| **3630.59** | O-H | Alcohol | stretch, free | strong, sharp |
| **3630.38** | | | | |
| **3677.54** | | | | |
| **3650.87** | | | | |
| **3620.92** | | | | |
| **3630.54** | | | | |
| **3589.60** | | | | |
| **3569.14** | | | | |
| **3385.80** | O-H | Alcohol | stretch, H bonded | strong, broad |
| **2925.28** | | | | |
| **2924.92** | | | | |
| **2924.70** | C-H | Alkane | stretch | strong |
| **2854.57** | | | | |
| **2854.75** | | | | |
| **2854.60** | | | | |
| **2345.89** | | | | |
| **2345.93** | C=O | Aliphatic Ketone | Stretching | -------- |
| **2345.75** | | | | |
| **1735.77** | | | | |
| **1774.14** | | | | |
| **1735.86** | | | | |
| **1719.33** | | | | |
| **1701.98** | C=O | Carbonyl | stretch | strong |
| **1701.95** | | | | |
| **1735.86** | | | | |
| **1719.44** | | | | |
| **1701.99** | | | | |
| **1686.08** | | | | |
| **1654.56** | C=O | Amide | stretch | strong |
| **1686.04** | | | | |
| **1654.45** | | | | |
| **1654.57** | | | | |
| **1647.94** | | | | |
| **1637.71** | N-H | Amide | bending | -------- |
| **1637.80** | | | | |
| **1637.42** | | | | |
| **1618.07** | | | | |
| **1618.11** | | | | |
| **1618.04** | N-H | Amide | bending | -------- |
| **1560.38** | | | | |
| **1542.35** | | | | |
| **1578.08** | | | | |
| **1560.38** | | | | |
| **1560.32** | | | | |
| **1542.34** | N-O | Nitro | stretch | strong, two bands |
| **1542.31** | | | | |
| **1508.35** | | | | |
| **1508.31** | | | | |
| **1508.35** | C=C | Aromatic | stretch | medium-weak, multiple bands |
| **1459.27** | | | | |
| **1458.83** | | | | |
| **1458.71** | | | | |
| **1377.58** | -C-H | Alkane | bending | variable |
| **1376.89** | | | | |
| **1376.50** | | | | |
| **1053.21** | C-O | Alcohol | stretch | strong |
| **722.32** | =C-H | Alkene | bending | strong |

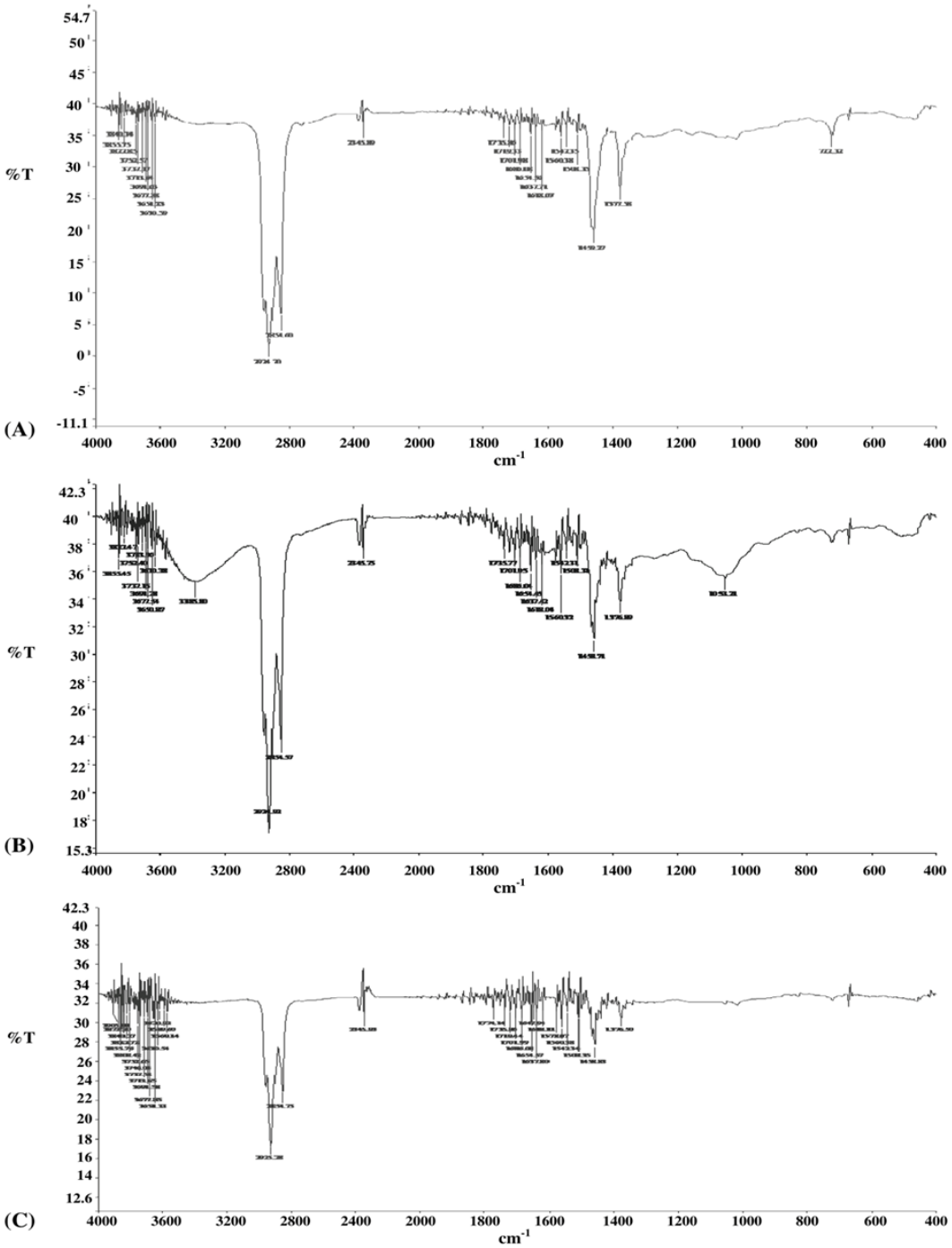


**Figure 9:** Fourier transform infrared spectra of CBLE.

## 4.2. Immunomodulatory activities

### 4.2.1. Effect of Plant Extract on Body Weight, Organs weight, Cellularity and the Leukocyte Count

Effect of different doses of *C. bonplandianus* leaf extracts in different organs on the basis of weight is shown in the Table 5**.** No significant changes in terms of increase or decrease in the body weight, liver weight and spleen weight were observed in mice that were fed with leaf extract for 20 days when compared with respective control groups.

**Table 5:** Effect of different doses of *C. bonplandianus* leaf extract (CBLE) on liver, spleen and body weights of mice after 20 days along with the phagocytic index (PI) of stimulation of phagocytosis assay.

| Group | Initial body weight | Final body weight | % body weight change | Liver weight | Rela-tive liver weight | Spleen weight | Relative Spleen weight | PI of yeast cell phago-cytosis |
|---|---|---|---|---|---|---|---|---|
| Control | 26.91 ± 0.95 | 30.04 ± 1.75* | 10.36 ± 2.05▲ | 4.75 ± 0.48 | 22.15 ± 0.80 | 0.67 ± 0.04 | 26.23 ± 0.92 | 63.85 ± 4.06 |
| CBL (50 mg/kg BW) | 25.53 ± 0.76 | 28.53 ± 1.08** | 10.48 ± 1.16▲ | 4.44 ± 0.59NS | 21.09 ± 0.74 | 0.59 ± 0.03* | 24.93 ± 0.75 | 70.51 ± 4.31NS |
| CBL (100 mg/kg BW) | 25.98 ± 1.20 | 28.83 ± 0.96** | 9.92 ± 1.15▲ | 3.87 ± 0.43* | 22.10 ± 0.78 | 0.68 ± 0.02NS | 25.29 ± 1.18 | 74.90 ± 4.18NS |
| CBL (250 mg/kg BW) | 25.35 ± 1.00 | 28.19 ± 0.55** | 10.11 ± 1.77▲ | 4.16 ± 0.30NS | 21.19 ± 0.98 | 0.60 ± 0.03NS | 24.74 ± 0.96 | 78.83 ± 4.98* |

NS $p > 0.05$, *$p < 0.05$, **$p < 0.01$, ***$p < 0.001$. Final body weight was compared with initial body weight of corresponding group and liver weight of treated groups was compared with liver weight of control group. ▲ represents increase.

**4.2.2. Assessment PFC assay and HA titer**

Humoral immune response modulate by CBLE is shown in Figure 10. In case of plaque forming cell assay the most significant value was found at 250 mg/kg BW dose compared to the control group. The highest visible agglutination was observed in case of HA titer assay (Table 6) at 100 mg/kg dose, followed by 250 and 50 mg/kg dose of CBLE when compared to the control.

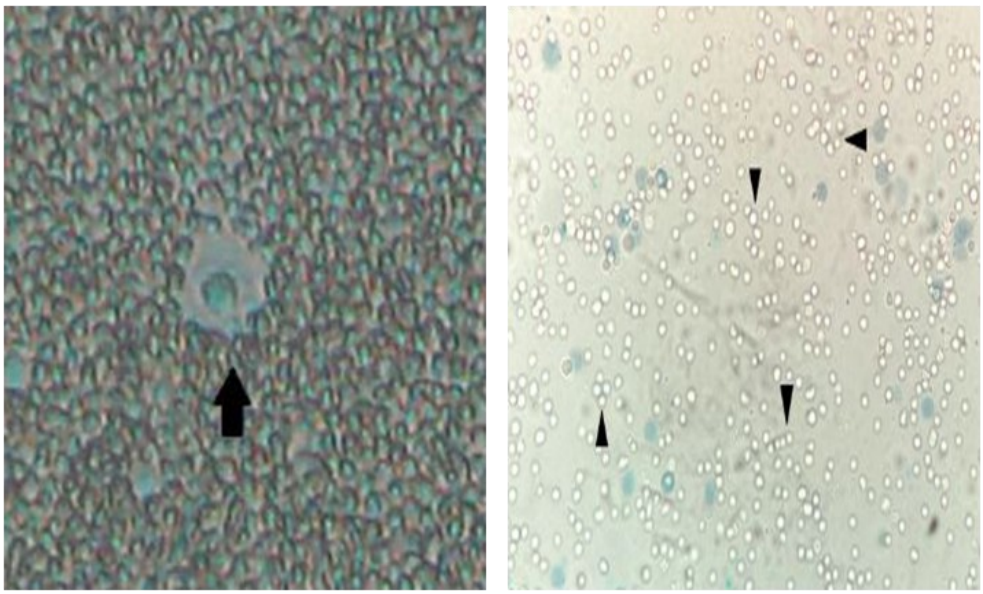

**Figure 10:** Photomicrograph of formation of plaques in the PFC assay. Antibody secreting cell in the centre, surrounded by sRBC lysis zone, formed due to IgM-complement complex. Photomicrograph (40 X) of viable murine splenic lymphocytes visualized using Trypan Blue staining.

**Table 6:** Summarizes the immunomodulatory effect of CBLE by Plaque Forming Cell (PFC) assay, Immunoglobulin M (IgM) levels and Hemagglutination (HA) titre assay.

| Group | PFC | IgM | HA Titre |
|---|---|---|---|
| Control | 107.13 ± 4.38 | 0.367 ± 0.05 | 1:40 |
| CBL (50 mg/kg BW) | 137.59 ± 5.41$^{*}$ | 0.53 ± 0.05$^{NS}$ | 1:40 |
| CBL (100 mg/kg BW) | 147.98 ± 5.023$^{*}$ | 0.59 ± 0.05$^{**}$ | 1:160 |
| CBL (250 mg/kg BW) | 157.97 ± 5.23$^{**}$ | 0.73 ± 0.06$^{*}$ | 1:80 |

$^{NS}$P>0.05, *P<0.05, **P<0.01 and ***P<0.001 vs control.

### 4.2.3. Immunoglobulin M (IgM) level

*In-vivo* IgM level is displayed in Table 6 and Figure 11 C. The IgM level at 0 mg/kg was 0.367 ± 0.05 mg/ml. At 250 mg/kg, the level of IgM was 0.73 ± 0.06 mg/ml. The dose-dependent correlation between PFC value and IgM level demonstrated high correlation between two inter-related parameters (Figure 11 D). The coefficient of determination ($R^2$) of PFC and IgM correlation for CBLE was 0.9533.

### 4.2.4. Counting of Peritoneal Macrophage

Stimulation of murine immune response was supported by elevation of peritoneal macrophage level with the increase in the dose of CBLE (Table 7). The most significant increase of the macrophage population was found at the dose of 250 mg/kg body weight (26.36 ± 0.97) in case of CBLE when compared with control groups.

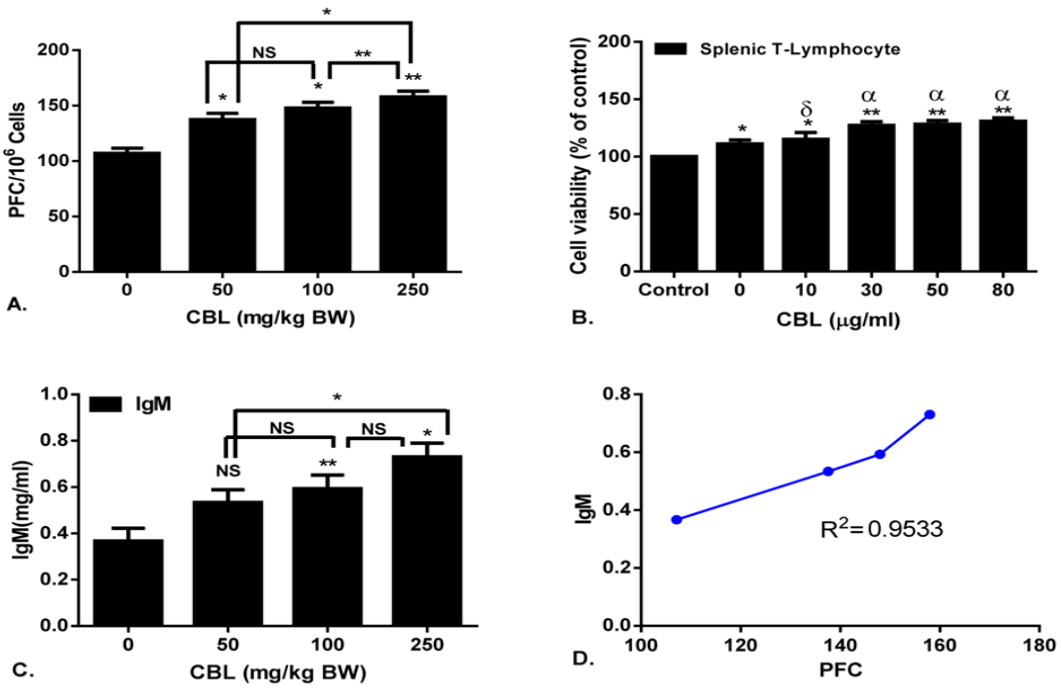


**Figure 11: A.** Increase in number of plaques in the PFC assay. **B.** Effect of CBLE on splenic lymphocyte viability. **C.** Dose dependent increase in total IgM expression. **D.** Correlation between PFC and IgM. [Where, R2 = coefficient of determination. N.S. = non-significant (P≥0.05), *P≤0.05, **P≤0.01, ***P≤0.001 versus group 1 (control) and α = P≤0.05 and δ = non-significant (P≥0.05) compared to the 0 µg/ml group.]

**Table 7:** Effect of different doses of *C. bonplandianus* leaf extract (CBLE) on total serum protein, albumin and globulin levels; splenocyte, leukocyte, and macrophage count after 20 days treatment.

| Group | Protein[a] | Albumin[a] | Globulin[a] | Spleenocyte[b] | Leukocyte[c] | Macro-phage[b] |
|---|---|---|---|---|---|---|
| Control | 5.73 ± 0.80 | 2.97 ± 0.52 | 3.43 ± 0.77 | 396.72 ± 8.25 | 9955.22 ± 249.59 | 17.51 ± 1.18 |
| CBL (50 mg/kg BW) | 6.57 ± 1.24$^{NS}$ | 4.01 ± 0.63$^{NS}$ | 4.53 ± 1.15$^{NS}$ | 424.01 ± 10.32$^{*}$ | 10696.37 ± 223.05$^{*}$ | 19.95 ± 1.38$^{NS}$ |
| CBL (100 mg/kg BW) | 8.92 ± 0.82$^{*}$ | 4.49 ± 0.79$^{*}$ | 5.95 ± 0.89$^{*}$ | 452.63 ± 8.94$^{*}$ | 11899.65 ± 193.13$^{**}$ | 24.08 ± 1.56$^{*}$ |
| CBL (250 mg/kg BW) | 10.30 ± 1.00$^{**}$ | 5.93 ± 0.33$^{*}$ | 6.99 ± 0.77$^{NS}$ | 474.28 ± 8.17$^{**}$ | 13023.62 ± 258.29$^{***}$ | 26.36 ± 0.97$^{*}$ |

a; Amount in g/dl, b; Mean ± SD × 106 cells per ml, c; Mean ± SD cells/mm3 N.S. Non significant, *P<=0.05, ** P<=0.01, *** P<=0.001; when compared with control.

**4.2.5. Cell proliferation assay**

The *in vitro* effect of CBLE on the murine splenic lymphocyte proliferation was showed in Figure 11 B. Cell viability of the con A stimulated group (0 CBLE µg/ml) was 111.00 ± 3.60 %when the cell viability of the control group was considered as 100 %. Cell viability at the highest dose (80 µg/ml) was 130.67 ± 3.06 %.

**4.2.6. Stimulation of the degree of Phagocytic Activity of Macrophages**

The effect of CBLE on the phagocytic capacity of murine peritoneal macrophage is illustrated in Figure 12 A. The phagocytic capacity was measured by mean percentage of macrophages engulfing >4 yeast cells. CBLE demonstrated significant increase (P<0.01) in phagocytic capacity at 250 mg/kg dose (39.62 ± 2.08) compared to 0 mg/kg dose (17.26 ± 1.25). Phagocytic index (PI) of CBLE on murine peritoneal macrophage is illustrated in Figure 12 B. The phagocytic index was calculated by multiplying the percentage of yeast-ingesting macrophages with the number of yeast-ingested per macrophages. Compared to 0 mg/kg, the PI of CBLE was significant (P<0.05) at 250 mg/kg dose (181.99 ± 7.04).

**4.2.7. Determination of Total Protein, Albumin, Globulin Levels in Serum**

Total serum protein, albumin and globulin levels poignantly increased with the increment in the doses of CBLE (Table 7). The protein, albumin and globulin level were significantly increased at 250 mg/kg body weight respectively 10.30 ± 1.00, 5.93 ± 0.33 and 6.99 ± 0.77 g/dl when compared with control group.

**4.2.8. Hemolytic activity**

The hemolytic activity of CBLE on murine erythrocytes was negligible when compared to the standard Titron X, as presented in the Figure 12 C. The percent of hemolysis increased in a dose dependent manner in case of CBLE.

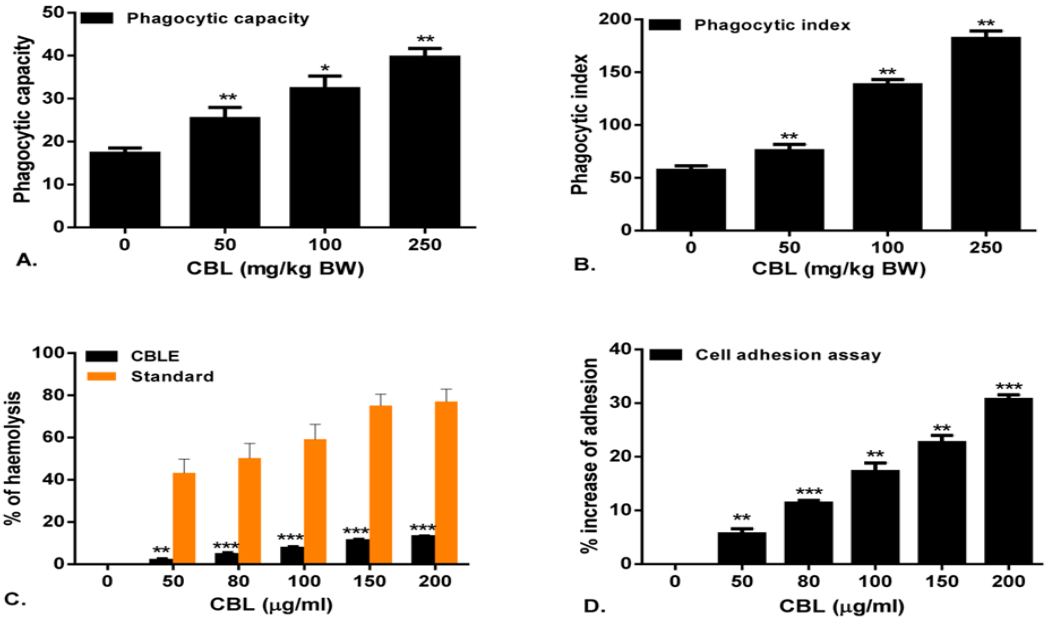


**Figure 12:** The effect of *C. bonplandianus* extracts on **A.** Phagocytic capacity and **B.** Phagocytic index of murine peritoneal exudate macrophages. **C.** Haemolytic activity **D.** In vitro cell adhesion assay. N.S. = non-significant (P≥0.05), *P≤0.05, **P≤0.01, ***P≤0.001 versus control.

**4.2.9. In Vitro Cell Adhesion Assay**

Adherence property of macrophages increased in a dose dependent manner with the increase in CBLE concentration (Figure 12 D). Percent increase of adhesion was increased in a dose dependent manner.

**4.2.10. Respiratory brust assay**

Increase of absorbance signifies increased respiratory burst activity (Figure 13 A). Significance increases in absorbance were observed at highest dose (200 µg/ml) when compared with control group (0 µg/ml).

**4.2.11. Inhibition of Lipopolysaccharide Induced Nitric Oxide Production**

The inhibition of NO production from LPS stimulated macrophage by CBLE is represented in Figure 13 B. The inhibition of NO is increased in a dose dependent manner for CBLE. The plant extract showed significant NO suppression capacity for each dose. At the highest concentration of 250 mg/kg body weight, the percentage of inhibition was 67.01 ± 3.96, which is very convincing.

**4.2.12. Myeloperoxidase release assay**

Significant (P<0.001) MPO reducing capacity (Figure 13 C) was observed in case of CBLE. At 200 µg/ml, the amount of reduction of MPO for CBLE was 25.54 ± 2.58 %.

**4.2.13. Carbon-Clearance assay**

The extent of removal of foreign particle through macrophage activity resulting in carbon clearance is expressed in terms of absorbance value. Lower absorbance value at 650 nm with increase in time represents clearance of the carbon particles from the

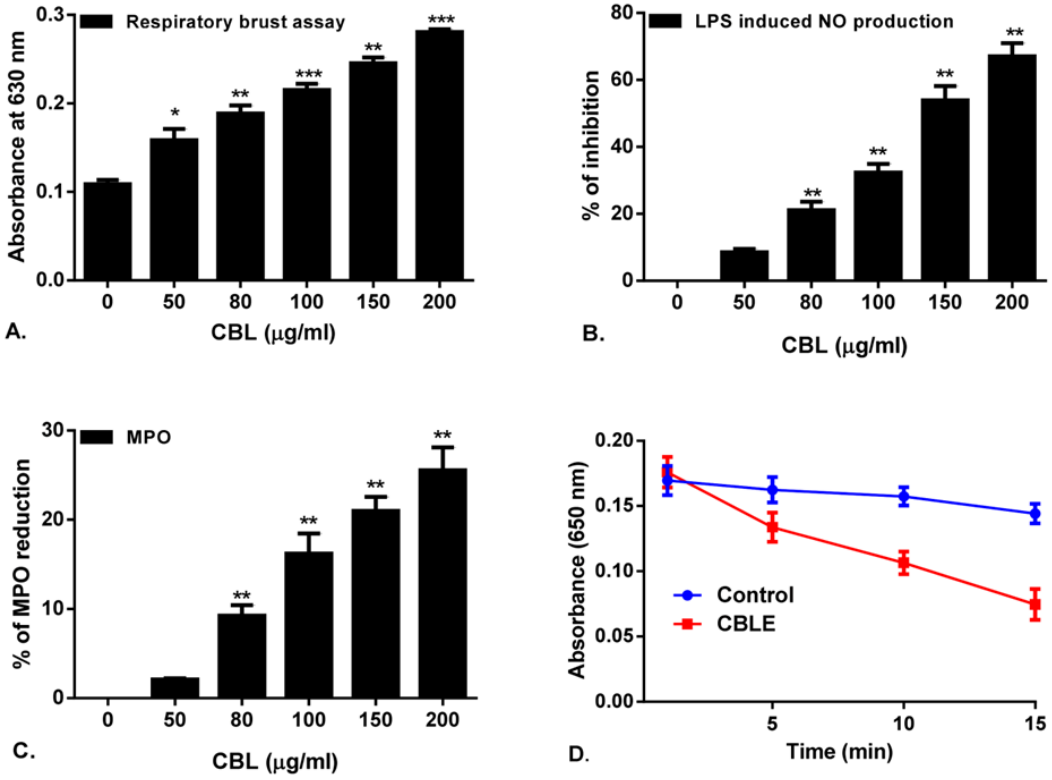


**Figure 13: A.** The respiratory burst activity of murine peritoneal exudates macrophages. **B.** Lipopolysacharide (LPS) induced nitric oxide production by CBLE. **C.** The percentage of MPO reduction by CBLE in murine peritoneal macrophages. **D.** Removal of non-specific carbon particles from the systemic circulation as evaluated by Carbon Clearance test.

central circulation. Figure 13 D displays the effect of CBLE on the carbon-clearance in murine model. In this present study, CBLE at 200 mg/kg dose demonstrated highest degree of carbon clearance activity at 15 min compared to the control group.

### 4.3. Anti-inflammatory activities

#### 4.3.1. Measurement of the inhibition of NO

The NO inhibitory capacity of CBLE is depicted in the Figure 15 B. NO expression of control was considered as 100 %. Gradual dose dependent decrease in NO expression was evident and at the highest dose the level of NO expression was 131.38 ± 9.53 % which was significantly ($P \leq 0.01$) lower than 0 µg/ml group.

#### 4.3.2. Estimation of cytokine expression

Cytokine expression was displayed in Figure 14 and 15. Expression of all cytokines were increased except TNF-a and IL-4 and the expression of IL-2 was significantly ($P \leq 0.001$) increased from 9.69 ± 0.68 pg/ml (control) to 57.78 ± 3.50 pg/ml (80 µg/ml). Expression of IFN-γ was also increased significantly ($P \leq 0.001$), from 68.38 ± 7.20 pg/ml (control) to 315.39 ± 14.61 pg/ml (80 µg/ml). The expression of IL-4 was decreased compared to control group. The level of IL

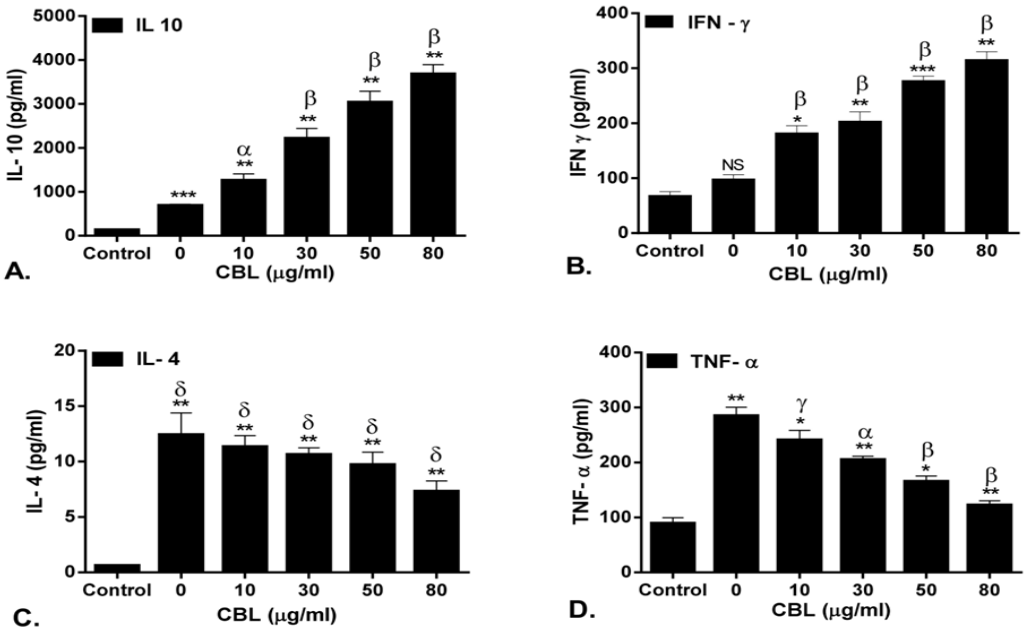


**Figure 14:** The effect of CBLE on Con A (5 µg/ml) stimulated **A.** IL-10, **B.** IFN-γ, **C.** IL-4 **D.** TNF-α release in murine lymphocytes. N.S. = non-significant (P≥0.05), *P≤0.05, **P≤0.01, ***P≤0.001 versus group 1 (control) and α = P≤0.05, β = P≤0.01, γ = P≤0.001 and δ = non-significant (P≥0.05) compared to the 0 µg/ml group.

-10 was elevated from129.54 ± 15.75 pg/ml (control) to 3679.65 ± 213.04 pg/ml (80 lg/ml). TNF-α significantly decrease at highest dose 80 µg/ml compared to control group 0 µg/ml. A major determinant of immunomodulatory activity was the ratio of IFN-γ/IL-4 which was also found to be elevated when increasing the CBLE dose form 0 to 80 µg/ml.

**4.3.3. Measurement of COX activities**

The effect of CBLE on the COX activity of murine splenic lymphocytes was displayed in Figure 16. Activity of both COX 1 and COX 2 was inhibited in a dose dependent manner with gradual increase in CBLE concentration. Inhibition of COX 1 and COX 2 resulting in suppression of total COX activity. At 0 µg/ml and 80 µg/ml (High dose), the total COX, COX 1 and COX 2 activities were 48.10 ± 2.99 U/ml (nmol/min/ml), 18.97 ± 1.48 U/ml and 29.13 ± 1.52 U/ml, and 26.07 ± 2.26 U/ml (nmol/min/ml), 13.22 ± 1.21 U/ml, 12.85 ± 1.51 U/ml respectively. Highly significant decrease in COX (P≤0.001) activity was found at the highest dose (80 µg/ml) when compared to the 0 µg/ml group.

**4.3.4. Inhibition of Prostaglandin E2**

CBLE has the potentiality to inhibit PGE2 synthesis in murine splenic lymphocytes was showed in Figure15 C and 15 D. Due to stimulation with Con A, PGE2 level was increased to 495.66 ± 24.49 pg/mL at 0 µg/ml, which was significantly down regulated ($P < 0.001$) to 142.58 ± 7.59 pg/mL at 80 µg/ml due to the effect of CBLE.

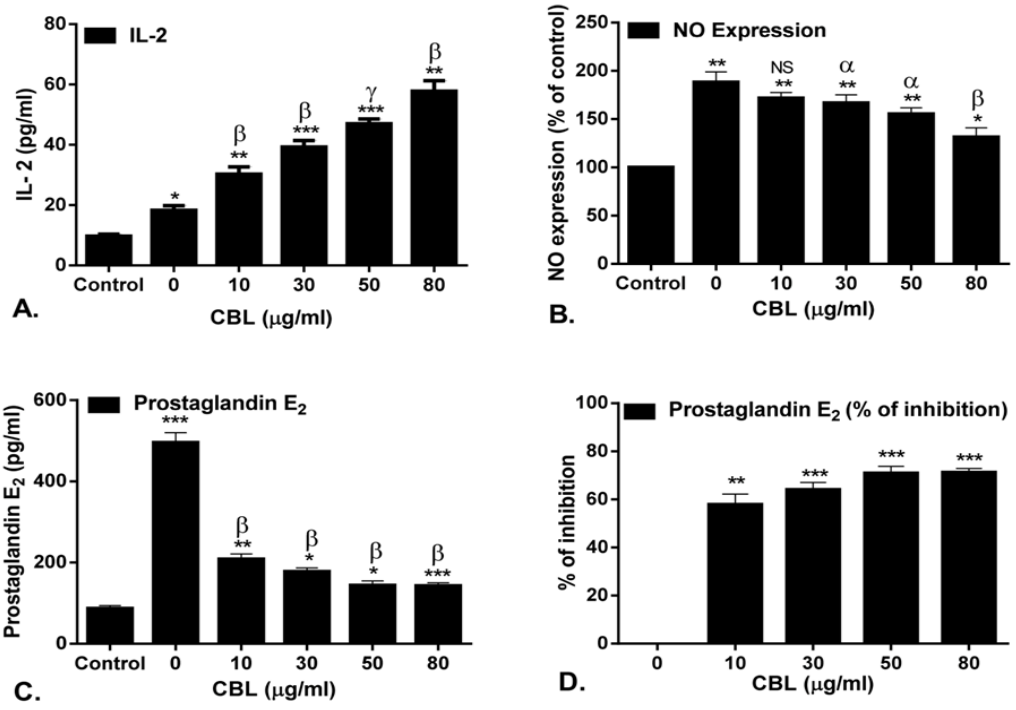


**Figure 15:** The effect of CBLE on Con A (5 µg/ml) stimulated **A.** IL-2 release in murine lymphocytes, **B.** NO Expression in murine lymphocytes, **C.** PGE2 level in murine lymphocytes **D.** Percentage of inhibition of PGE2 level. N.S. = non-significant (P≥0.05), *P≤0.05, **P≤0.01, ***P≤0.001 versus group 1 (control) and α = P≤0.05, β = P≤0.01, γ = P≤0.001 and δ = non-significant (P≥0.05) compared to the 0 µg/ml group.

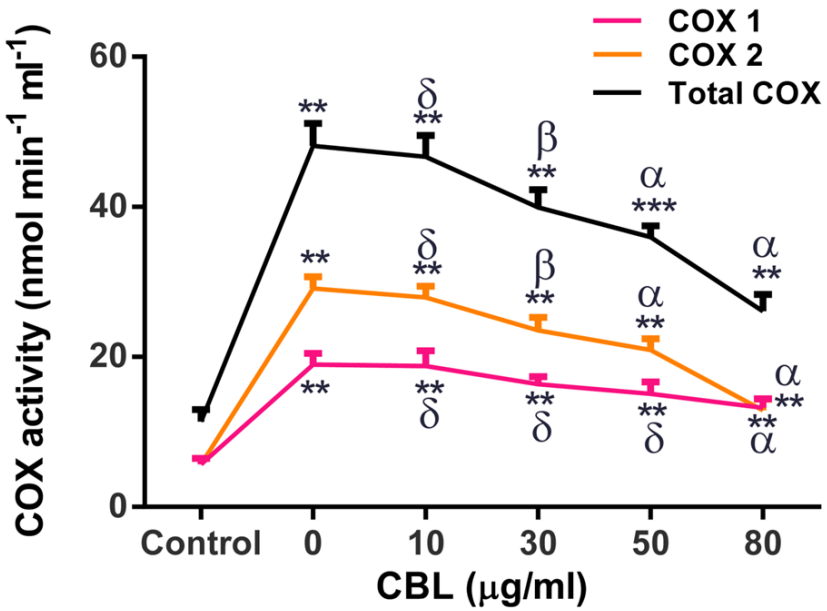


**Figure 16:** The effect of CBLE on Con A (5 µg/ml) stimulated COX-1, COX-2 and total COX activities in murine lymphocytes. N.S. = non-significant (P≥0.05), *P≤0.05, **P≤0.01, ***P≤0.001 versus group 1 (control) and α = P≤0.05, β = P≤0.01, γ = P≤0.001 and δ = non-significant (P≥0.05) compared to the 0 µg/ml group.

### 4.3.5. Correlation study

Correlation analysis between all the cytokines (Figure 17, 18, 19) revealed that the expression of IL-10 was highly correlated with expression of IL-2, where both the cytokines were up-regulated and high negative correlation of IL-2 resided with TNF-a. Correlations between the expression of different cytokines and NO were displayed in Figure 20, 21, where a highly negative correlation was found between IFN-γ and NO. The linear correlation analyses between the PGE2 levels with different cutokines are demonstrated in Figure 22, 23. High positive correlation was observed between PGE2 level with COX-1 and COX-2 activities. The highest degree of correlation was found between PGE2 and IL-2 level.

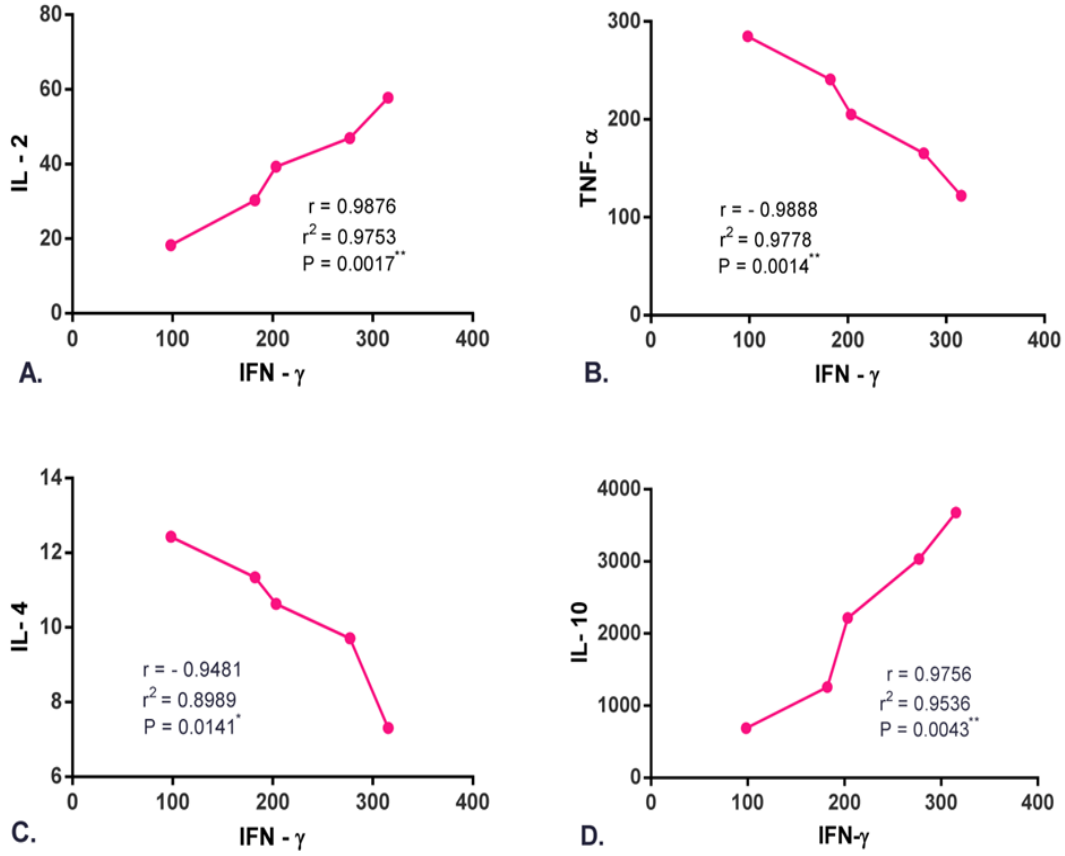


**Figure 17:** Correlation between the expressions of **A.** IL-2 versus IFN-γ; **B.** TNF-a versus IFN-γ; **C.** IL-4 versus IFN-γ; **D.** IL-10 versus IFN-γ. Axes 'x' and 'y' denote correlation points of respective cytokines measured at pg/ml at different doses of CBLE (0–80 µg/ml). Where, $R^2$ = coefficient of determination.

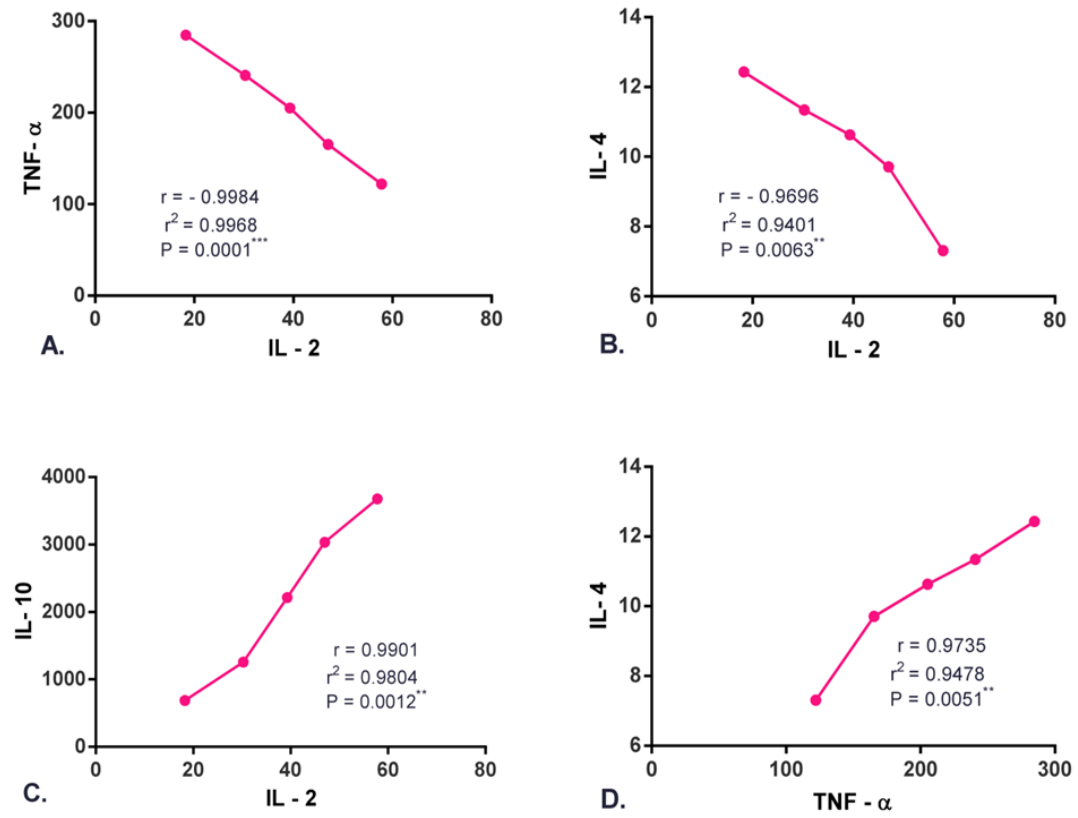


**Figure 18:** Correlation between the expressions of **A.** TNF-a versus IL-2; **B.** IL-4 versus IL-2; **C.** IL-10 versus IL-2 and **D.** IL-4 versus TNF-a. Axes 'x' and 'y' denote correlation points of respective cytokines measured at pg/ml at different doses of CBLE (0–80 µg/ml). Where, $R^2$ = coefficient of determination.

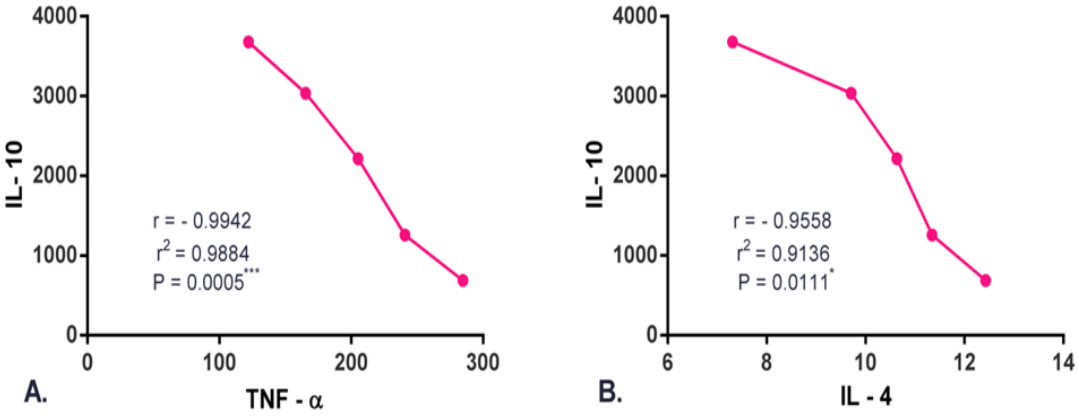


**Figure 19:** Correlation between the expressions of **A.** IL-10 versus TNF-α and **B.** IL-10 versus IL-4. Axes 'x' and 'y' denote correlation points of respective cytokines measured at pg/ml at different doses of CBLE (0–80 µg/ml). Where, $R^2$ = coefficient of determination.

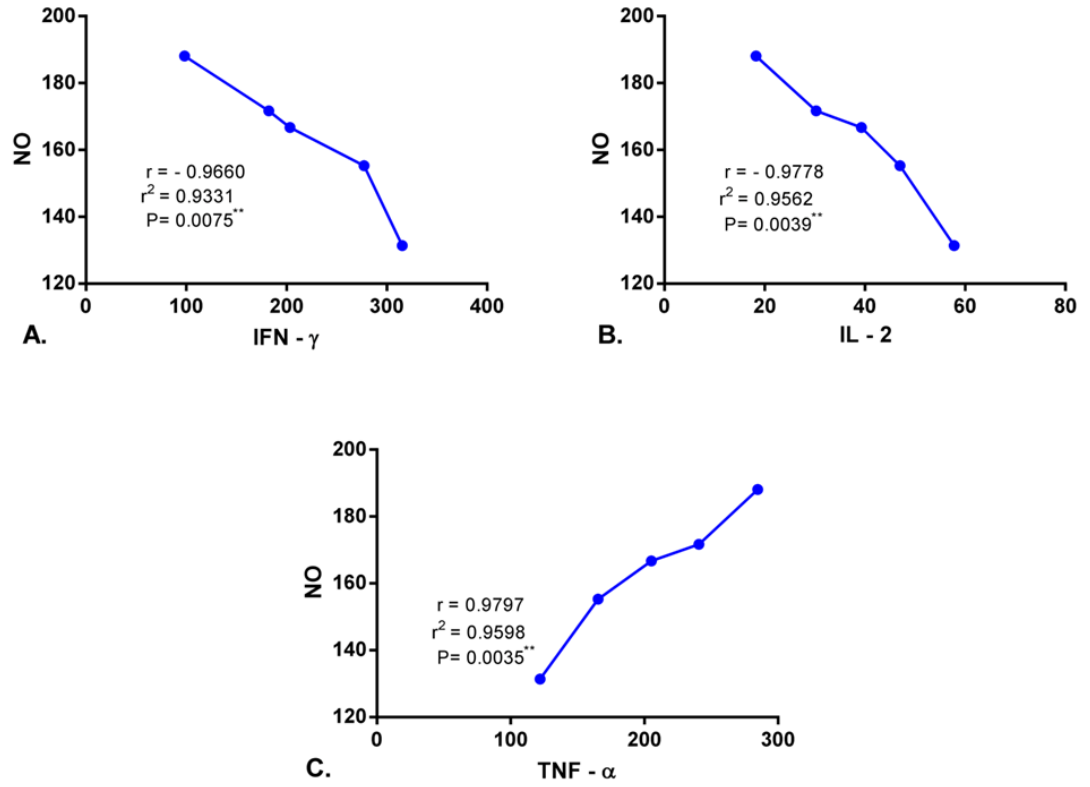


**Figure 20:** Correlation of NO with **A.** IFN-γ; **B.** IL-2; **C.** TNF-α expression under the influence of CBLE. Axes 'x' and 'y' denote correlation points of respective cytokines measured at pg/ml and NO levels at different doses of CBLE (0–80 lg/ml). Where, $R^2$ = coefficient of determination.

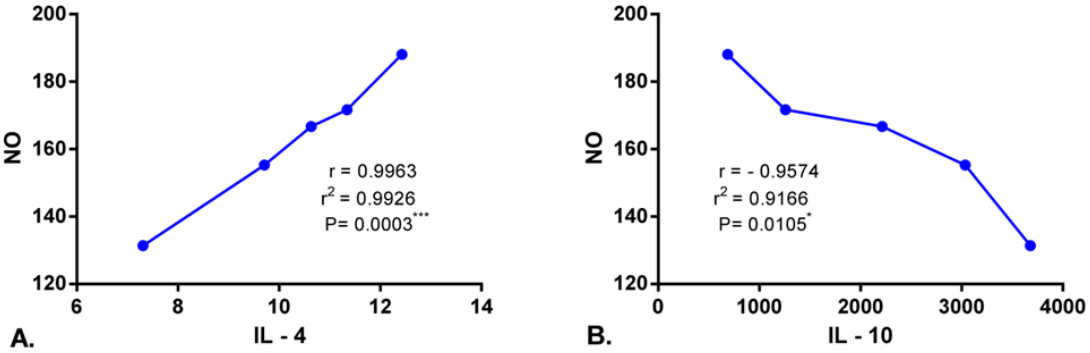


**Figure 21:** Correlation of NO with **A.** IL-4 and **B.** IL-10 expression under the influence of CBLE. Axes 'x' and 'y' denote correlation points of respective cytokines measured at pg/ml and NO levels at different doses of CBLE (0–80 lg/ml). Where, $R^2$ = coefficient of determination.

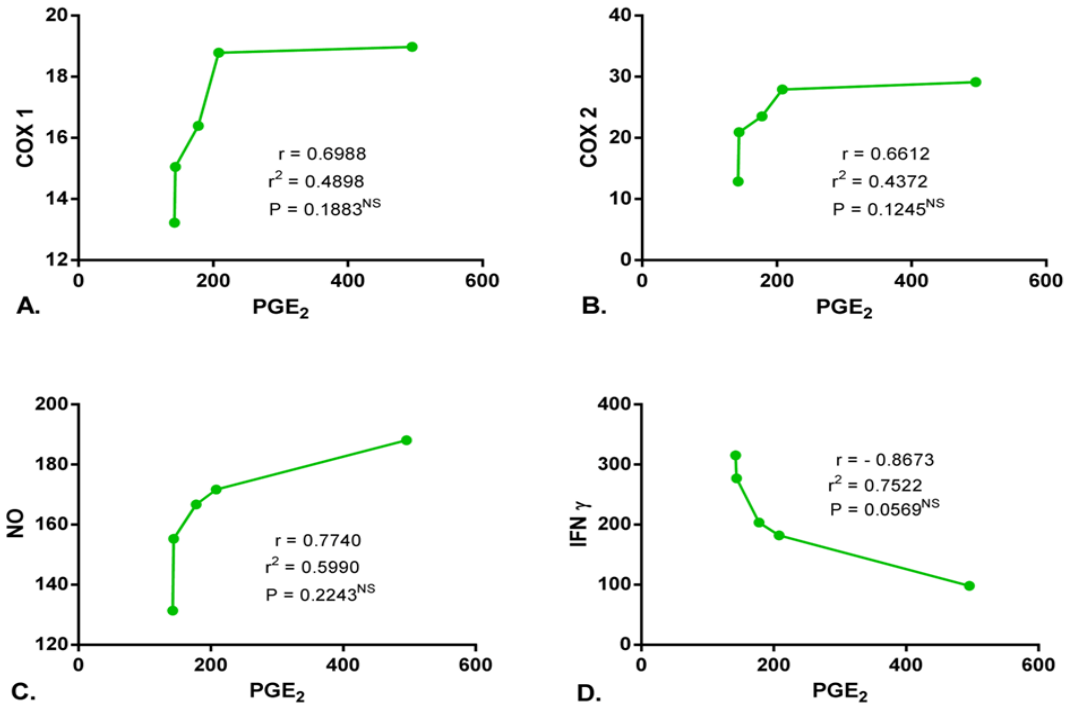


**Figure 22:** Correlation of prostaglandin E2 level with the expression of different pro- and anti-inflammatory mediators. An ax "x" and "y" denotes correlation points of respective parameters measured at pg/mL at different dose of CBLE (0–80 µg/mL). Where, $R^2$ = coefficient of determination.

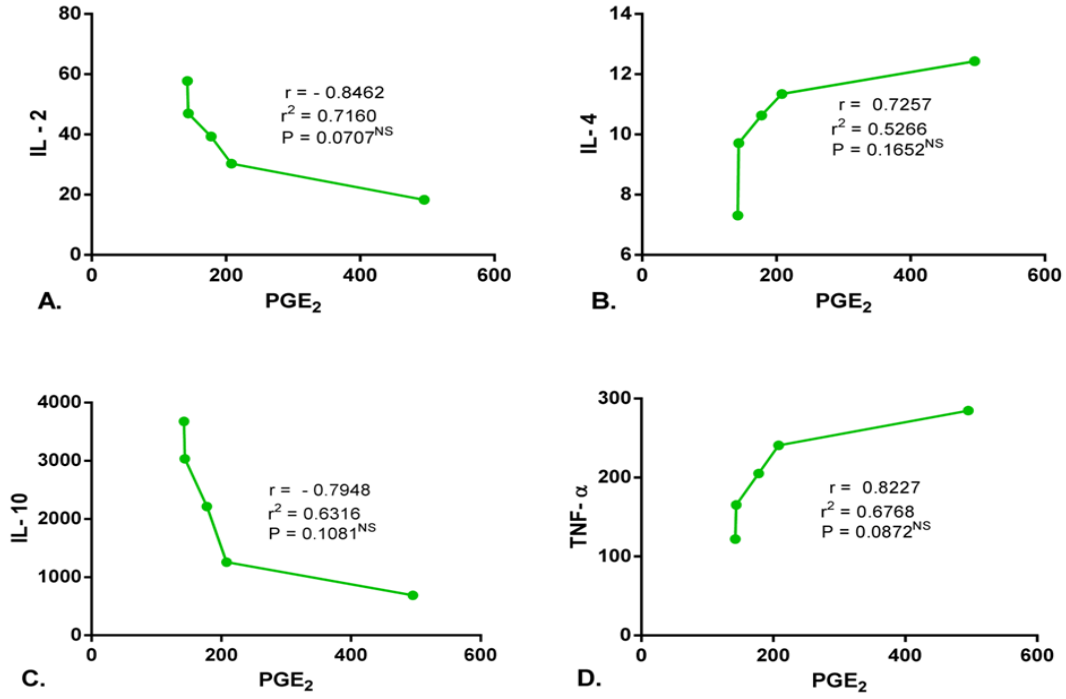


**Figure 23:** Correlation of prostaglandin E2 level with the expression of different pro- and anti-inflammatory mediators. An ax "x" and "y" denotes correlation points of respective parameters measured at pg/mL at different dose of CBLE (0–80 µg/mL). Where, $R^2$ = coefficient of determination.

### 4.3.6. Molecular Docking

The bioactive compounds of *Croton bonplandianus* was checked for possible interactions with several proteins playing the essential role in different immunogenic pathways of humans and other major vertebrates. These proteins acted as receptors required for molecular docking experiments. The ligands required to conduct the experiment are the compounds identified my GC-MS analysis of the plant extract. Upon a series of receptor-ligand interaction study, it is seen that α-amyrin has the highest interaction with all the receptors on an average followed by Ethyl iso-allocholate (Figure 24). On the other hand Octadecanoic acid has the least binding affinity with the receptors.. The highest binding affinity was found between α-amyrin and a protein with PDB ID 1cqe which is the crystal structure of prostaglandin (Figure 25,26). The molecular surface view shows that the phytochemical fits perfectly inside the binding pocket of prostaglandin molecule (Figure 26). The association between prostaglandin and the amino acids (Figure 25) and the low energy of binding between the two hints a stable conjugation. Such kind of association is can alter the regulation of metabolic response arose by immune response.

| | 1cqe | 1hik | 1tnf | 2h24 | 6cox |
|---|---|---|---|---|---|
| 1_Octacosanol | -4.2 | -3.3 | -3.1 | -4.4 | -4.9 |
| 17_Pentatriacontene | -5.4 | -3.8 | -3.4 | 4.9 | -4.7 |
| Amyrin | -10.3 | -7.6 | -7.5 | -9.2 | -9.1 |
| Ascorbic acid | -6 | -5.4 | -5.9 | -4.4 | -6.9 |
| Campesterol | -9.1 | -5.2 | -6.1 | -8.4 | -7.3 |
| Eicosanoic acid | -4.8 | -2.8 | -3.2 | -4.5 | -5 |
| Ethanol_ 2_ (octadecyloxy) | -4.4 | -3.6 | -3.1 | -4.2 | -4.6 |
| Ethyl iso_allocholate | -9 | -7 | -9.3 | -7.1 | -8.5 |
| Hentriacontane | -5.3 | -3.7 | -2.7 | -4.9 | -4.4 |
| N-Hexadecanoic acid | -4.1 | -3.6 | -3.2 | -3.7 | -5 |
| Octadecanoic acid | -4.6 | -2.7 | -3.4 | -4.9 | -4.8 |
| Phytol | -5.2 | -3.9 | -3.6 | -4.2 | -5.6 |
| Ribitol | -4.9 | -4.5 | -5.1 | -3.8 | -5.8 |
| Squalene | -6.5 | -5.9 | -4 | -6.5 | -6.8 |
| Stigmasterol | -8.4 | -5.6 | -6.2 | -9.2 | -7.9 |
| A-Tocopherol | -8.1 | -5.9 | -5 | -7.2 | -8.6 |
| B-Sitosterol | -8.2 | -5.6 | -5.9 | -8 | -9.2 |

HIGH LOW

**Figure 24:** Heatmap based on binding energy among proteins and phytochemicals. The phytochemicals which served as ligands for molecular docking experiment are along the Y axis and the proteins are placed on the X-axis.

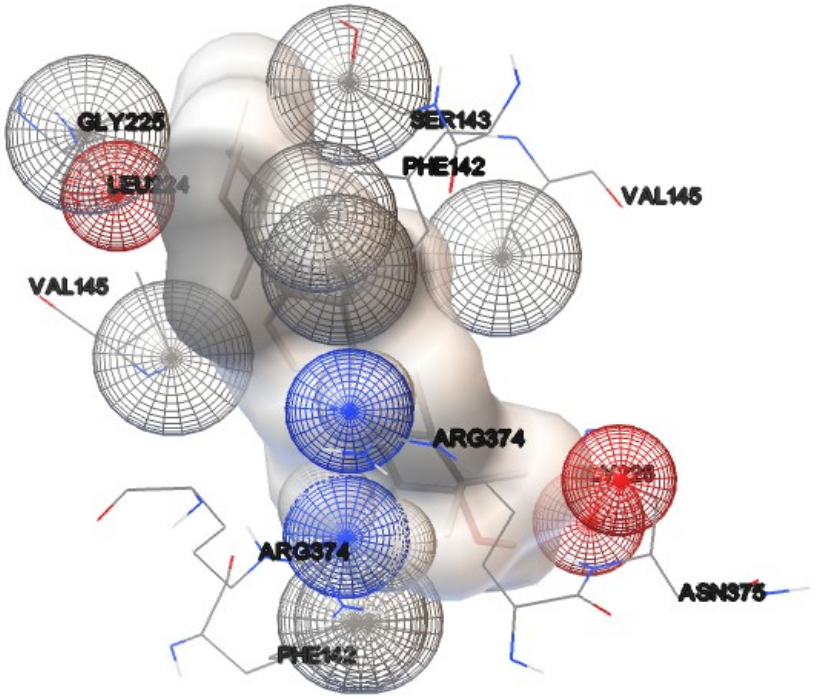


**Figure 25:** Molecular docking between prostaglandin protein and α-amyrin.

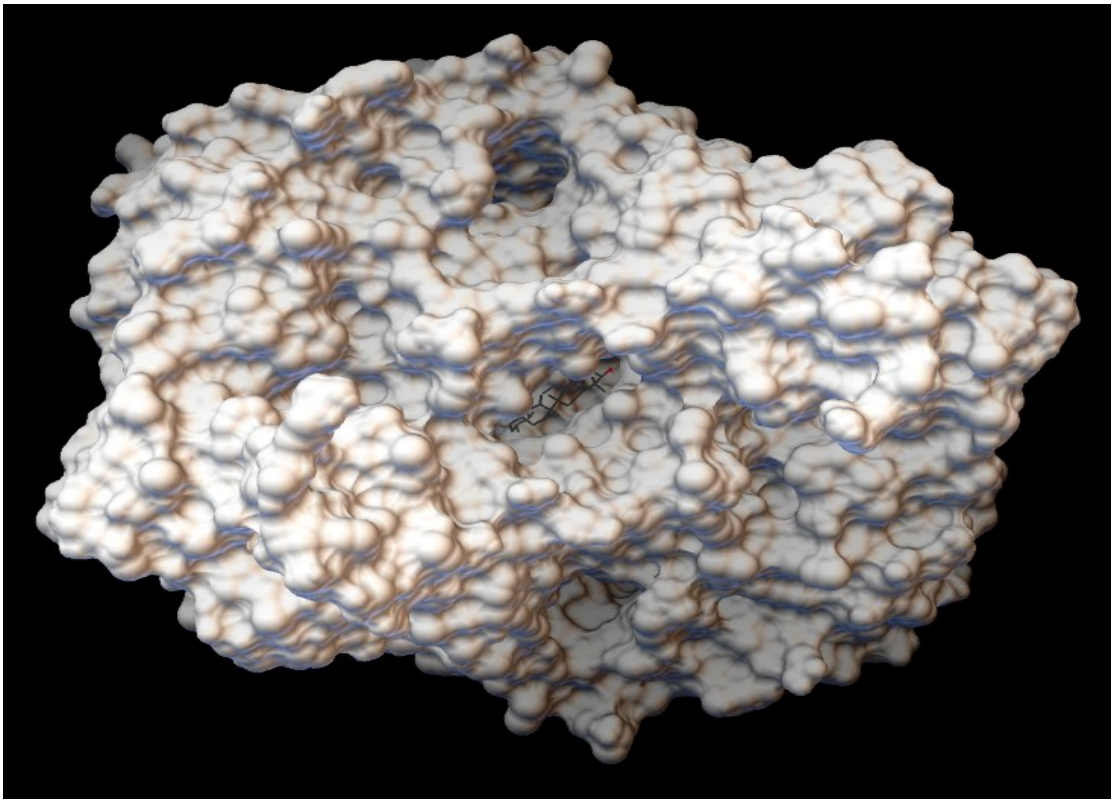

**Figure 26:** Molecular docking (molecular surface view) between prostaglandin protein and α-amyrin.

### 4.4. Antioxidant and free radical scavenging activities

The free radical scavenging activity of CBL in dose dependent manner and the differences in the activities compared with standard compound. Half maximal inhibitory concentration ($IC_{50}$) of CBL and corresponding references are shown in the Table 8.

#### 4.4.1. Total antioxidant activity

At 200 µg/ml the percentage of inhibition (Figure 29) for CBLE and standard ascorbic acid were 84.15±0.53 and 69.29±0.07 respectively with an $IC_{50}$ value of 46.57±2.19 and 116.46±5.91 respectively.

#### 4.4.2. DPPH radical scavenging activity

At 20 µg/ml the percentage of inhibition (Figure 27) for CBLE and standard ascorbic acid were 90.13±0.86 and 87.40±5.04 respectively with an $IC_{50}$ value of 3.79±0.06 and 10.49±0.77 respectively.

#### 4.4.3. Hydroxyl radical scavenging activity

The percentage of inhibition (Figure 27) of hydroxyl radical scavenging for CBLE and standard mannitol at 200 µg/mL were 70.56±2.33 and 31.31±0.84 with an $IC_{50}$ value of 173.65±4.96 and 597.15±11.90 respectively.

#### 4.4.4. Superoxide radical scavenging activity

At 50 µg/mL the percentage of inhibition for CBLE and standard quercetin (Figure 31) were 60.29±1.83 and 39.46±1.46 respectively with an $IC_{50}$ value of 44.69±1.90 and 94.59±3.75.

#### 4.4.5. Nitric oxide scavenging activity

The percentage of inhibition of NO scavenging for CBLE and standard curcumin (Figure 32) at 75 µg/mL were 59.82±2.86 and 34.98±1.67. The $IC_{50}$ value of CBLE and curcumin were 36.74±2.79 and 129.82±7.31 respectively.

**Table 8:** $IC_{50}$ values of *Croton bonplandianus* (CBL) and standard for different antioxidant and free radical scavenging assays.

| Antioxidant Parameters | CBL | Standard |
|---|---|---|
| **DPPH** | 3.79±0.06** | 10.49±0.77 (Ascorbic Acid) |
| **Hydroxyl Radical** | 173.65±4.96*** | 597.15±11.90 (Mannitol) |
| **Hydrogen Peroxide** | 222.95±11.53** | 2185.22±187.45 (Sodium Pyruvate) |
| **Nitric Oxide** | 36.74±2.79*** | 129.82±7.31 (Curcumin) |
| **Superoxide Anion** | 44.69±1.90*** | 94.59±3.75 (Quercetin) |
| **Hypochlorous Acid** | 66.58±4.39** | 117.50±10.02 (Ascorbic Acid) |
| **Total Antioxidant Activity** | 46.57±2.19** | 116.46±5.91 (Ascorbic Acid) |
| **Peroxynitrite** | 785.48±59.32*** | 785.84±59.75 (Gallic Acid) |
| **Singlet Oxygen** | 257.00±3.22*** | 48.41±2.02 (Lipoic Acid) |
| **Lipid Peroxidation** | 19.70±1.32** | 11.16±0.26 (Trolox) |
| **Iron Chelation** | 123.46±1.92*** | 10.23±0.89 (EDTA) |

Units in µg/ml. Data expressed as mean ± S.D (n=6). *p<0.05; **p<0.01; ***p<0.001; NS – Non significant when compared with standard.

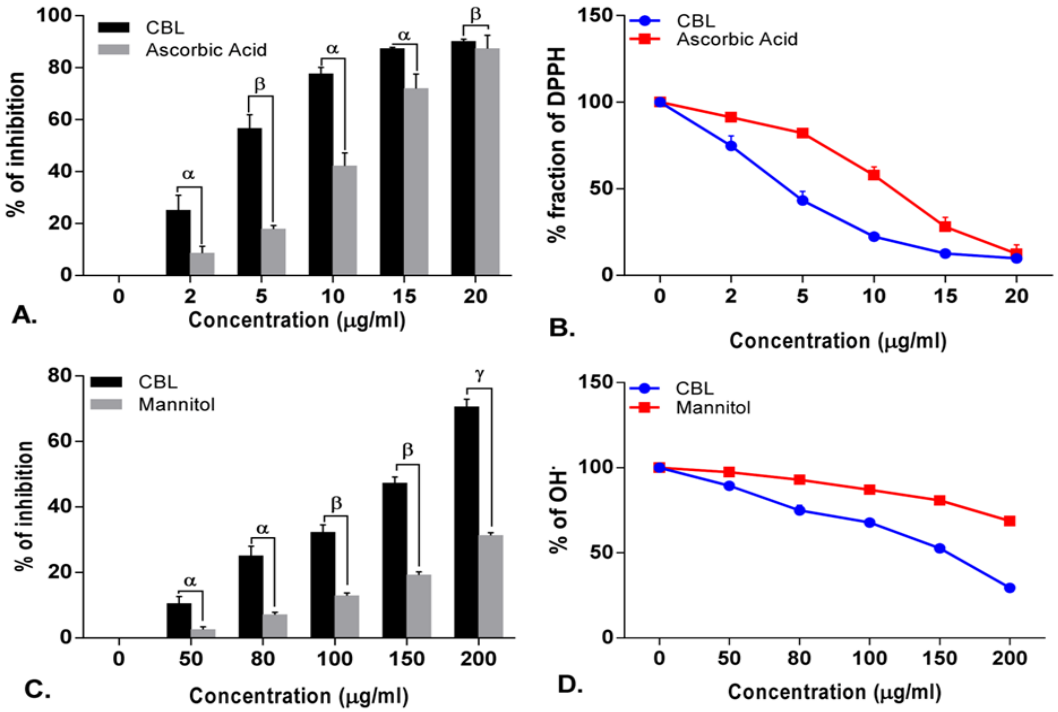


**Figure 27:** Antioxidant activity of *Croton bonplandianus*. **(A)** & **(B)** DPPH scavenging activity; **(C)** % of hydroxyl radical ($OH^{\bullet}$) scavenging Vs standard mannitol; **(D)** depicts remaining unneutralized $OH^{\bullet}$. Data expressed as mean ± S.D (n=6). $^{\alpha}p<0.05$; $^{\beta}p<0.01$; $^{\gamma}p<0.001$; $^{NS}$-Non significant when compared with standard.

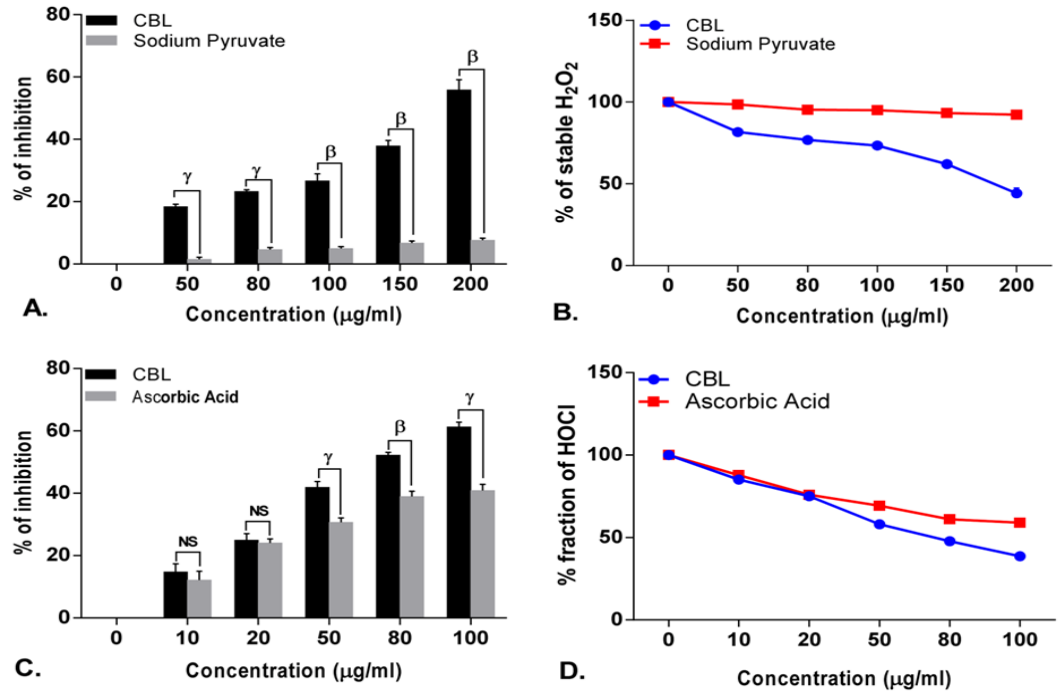


**Figure 28:** Antioxidant activity of *Croton bonplandianus*. **(A)** % of inhibition of hydrogen peroxide ($H_2O_2$)Vs standard sodium pyruvate; **(B)** depicts remaining unneutralized $H_2O_2$; **(C)** % inhibition of Hypochlorous acid (HOCl) Vs standard ascorbic acid; **(D)** depicts unneutralized HOCl radicals. Data expressed as mean ± S.D (n=6). α p<0.05; β p<0.01; γ p<0.001; NS-Non significant when compared with standard.

**4.4.6. Hydrogen peroxide scavenging activity**

At 200 µg/ml the percentage of inhibition for CBLE and standard sodium pyruvate (Figure 28) were 55.81±3.27 and 7.64±0.68 respectively with an $IC_{50}$ value 222.95±11.53 and 2185.22±187.45 respectively.

**4.4.7. Peroxynitrite scavenging activity**

The percentage of inhibition of $OONO^-$ scavenging for CBLE and standard gallic acid (Figure 32) at 200 µg/mL were 19.59±1.40 and 17.68±0.21 respectively with an $IC_{50}$ value of 785.48±59.32 and 785.84±59.75 respectively.

**4.4.8. Singlet oxygen scavenging activity**

At 200 µg/ml the percentage of inhibition for CBLE and standard lipoic acid (Figure 31) were 51.580000±0.370000 and 77.980000±0.3459769. The $IC_{50}$ values were 257.00±3.22 and 48.41±2.02 respectively.

**4.4.9. Hypochlorous acid scavenging activity**

The percentage of inhibition of HOCL scavenging for CBLE and standard ascorbic acid (Figure 28) at 100 µg/ml were 38.66±1.50 and 59.09±1.92. The $IC_{50}$ values were 66.58±4.39 and 117.50±10.02 respectively.

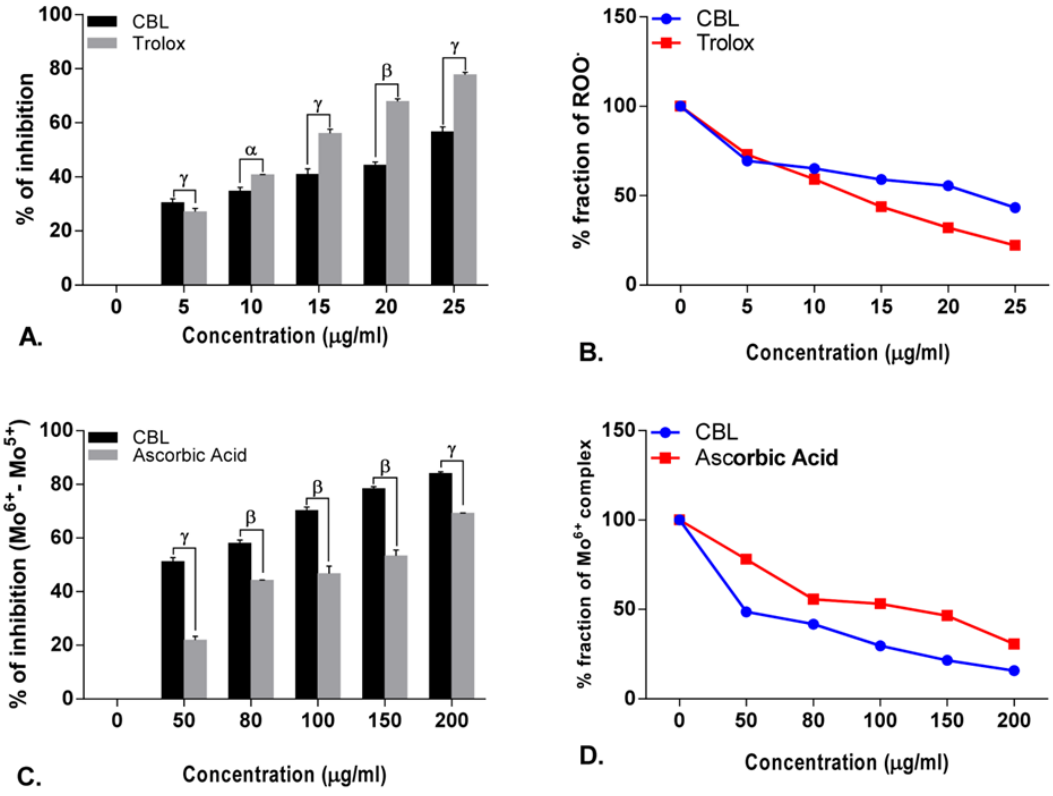


**Figure 29:** Antioxidant activity of *Croton bonplandianus*. **(A)** % inhibition of lipid peroxidation Vs standard trolox; **(B)** depicts remaining unneutralized lipid peroxides ($ROO^{\bullet}$); **(C)** & **(D)** concentration dependent Total antioxidant activity and extent of $Mo^{6+}$ reduction;. Data expressed as mean ± S.D (n=6). α $p<0.05$; β $p<0.01$; γ $p<0.001$; NS-Non significant when compared with standard.

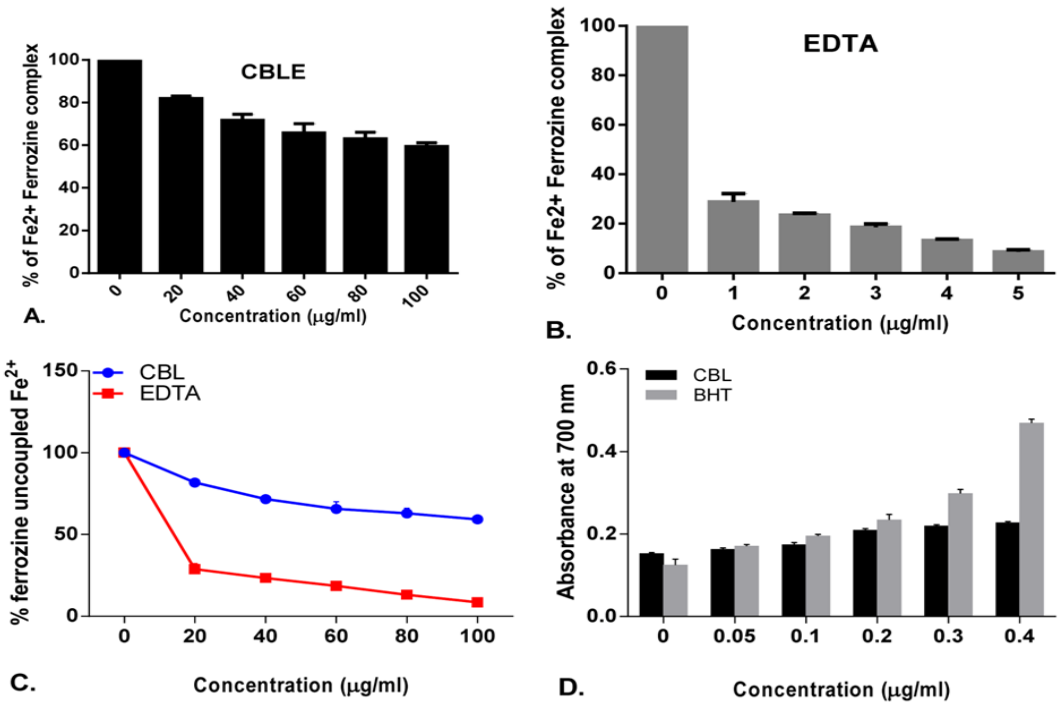


**Figure 30:** Antioxidant activity of *Croton bonplandianus*. (**A** and **B**) $Fe^{2+}$-chelation Vs standard EDTA; **(C)** depicts remaining unneutralized $Fe^{2+}$; **(D)** Total reducing power activity. Data expressed as mean ± S.D (n=6). α $p<0.05$; β $p<0.01$; γ $p<0.001$; NS-Non significant when compared with standard.

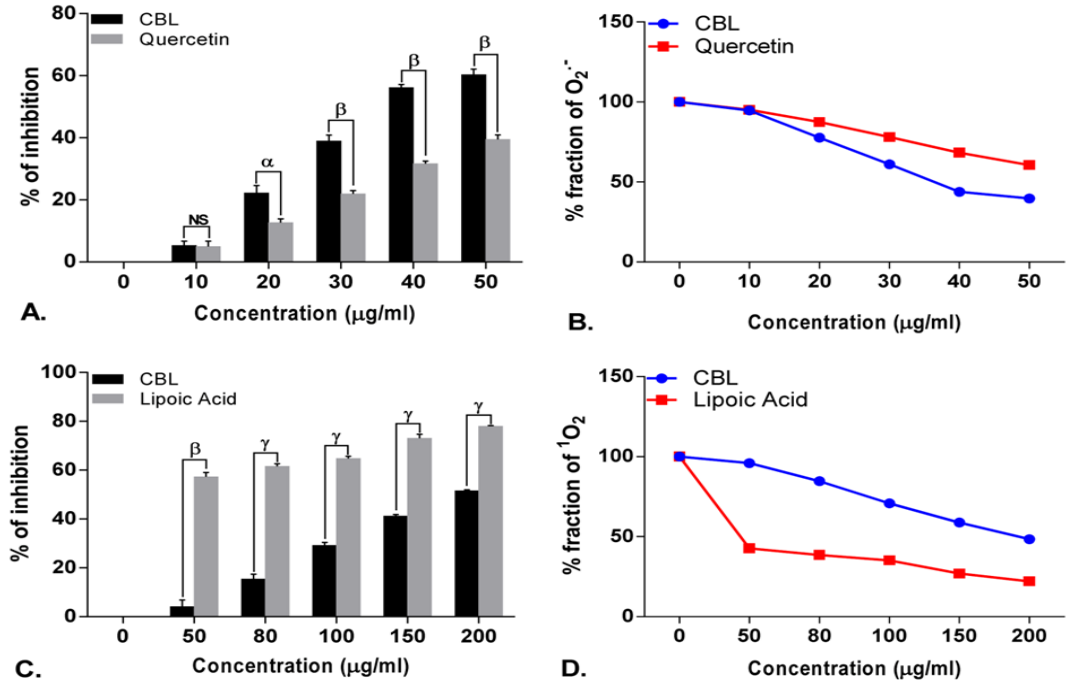


**Figure 31:** Antioxidant activity of *Croton bonplandianus*. **(A)** % inhibition of Superoxide ($O_2^{\bullet-}$) Vs standard quercetin; **(B)** depicts unneutralized superoxide ($O_2^{\bullet-}$) radicals. **(C)** % inhibition of Singlet $O_2$ ($^1O_2$) Vs standard lipoic acid; **(D)** depicts unneutralized Singlet $O_2$ ($^1O_2$). Data expressed as mean ± S.D (n=6). α $p<0.05$; β $p<0.01$; γ $p<0.001$; NS-Non significant when compared with standard.

**4.4.10. Iron chelating activity**

At 100 µg/ml the percentage of $Fe^{2+}$-ferrozine complex for CBLE were 59.36±1.80 (Figure 30). The percentage of Fe2+ -ferrozine complex for standard EDTA was 8.59±0.90. The $IC_{50}$ values were 123.46±1.92 and 10.23±0.89.

**4.4.11. Reducing power assay**

Increase in absorbance value at 700 nm denotes higher reducing power (Figure 30). At 0.4 mg/ml, the absorbance value of CBLE and BHT acid were 0.22±0.01 and 0.46±0.01 respectively.

**4.4.12. Inhibition of lipid peroxidation activity**

The percentage of inhibition of lipid peroxidation for CBLE and standard trolox (Figure 29) were 56.68±1.79 and 77.81±0.90. The $IC_{50}$ values were 19.70±1.32 and 11.16±0.26 respectively.

**4.4.13. Determination of phenol and flavonoid content in CBL extract**

Total amount of phenoloic content present in the hydromethanolic extract of CBL was found to be 75.06 ± 2.33 mg/ml gallic acid equivalent per 100 mg plant extract and the total flavonoid content of CBL extract was 52.17 ± 4.36 mg/ml quercetin equivalent per 100 mg plant extract.

**4.4.14. Differential effects on the individual components of Haber–Weiss reaction (Fenton chemistry)**

The Fenton chemistry as a part of the Haber-Weiss reactions is considered central to the intracellular free radical formation cascade. *C. bonplandianus* extract was evaluated for their capacity to directly affect the individual components of the Haber–Weiss reaction. *C. bonplandianus* demonstrated significantly $H_2O_2$ neutralizing activity (Figure 30 A). The ferric iron ($Fe^{2+}$) chelation capacity of *C. bonplandianus* at 200 µg/mL was 59.36 ± 1.81 % (Figure 30 B). EDTA, however demonstrated significantly ($P<0.001$) superior ferric chelation capacity as demonstrated by its low $IC_{50}$ value of 10.23±0.89 µg/ml. In case of direct scavenging of $OH^{\bullet}$, *C. bonplandianus* demonstrated superior activity than that of the standard mannitol.

**4.4.15. Inhibition of $OH^{\bullet}$: bivariate analysis**

Dose-dependent bivariate correlation analysis of $Fe^{2+}$ chelation and $H_2O_2$ inhibition were performed vs inhibition of $OH^{\bullet}$ in order to reflect how individually *C. bonplandianus* may inhibit the formation of $OH^{\bullet}$. $Fe^{2+}$ chelation activity by the inhibition of $OH^{\bullet}$ is higher in the presence of *C. bonplandianus* ($r = 0.8925$ and $r^2 = 0.7966$). The correlation between the inhibitions of $OH^{\bullet}$ and $H_2O_2$ were much more comparable, with minor trend towards $H_2O_2$ mediated effect ($r = 0.9825$ and $r^2 = 0.9652$) (Figure 33A and 33B).

## 4.5. Hepatoprotective activities

**4.5.1. Acute toxicity study**

CBL extract was administrated to the experimental animals up to 2,000 mg/kg body weight. However, at the 2000 mg/kg

body weight dose, no sign of mortality and physiological deformation were observed in the experimental animals. Therefore, 50 mg/kg BW, 100 mg/kg BW and 250 mg/kg BW doses were selected as a low, medium and high dose in the *in vivo* hepatoprotective experiments.

### 4.5.2. Body and liver weight

Significant body weight changes were observed in $CCl_4$, CBLE and silymarin

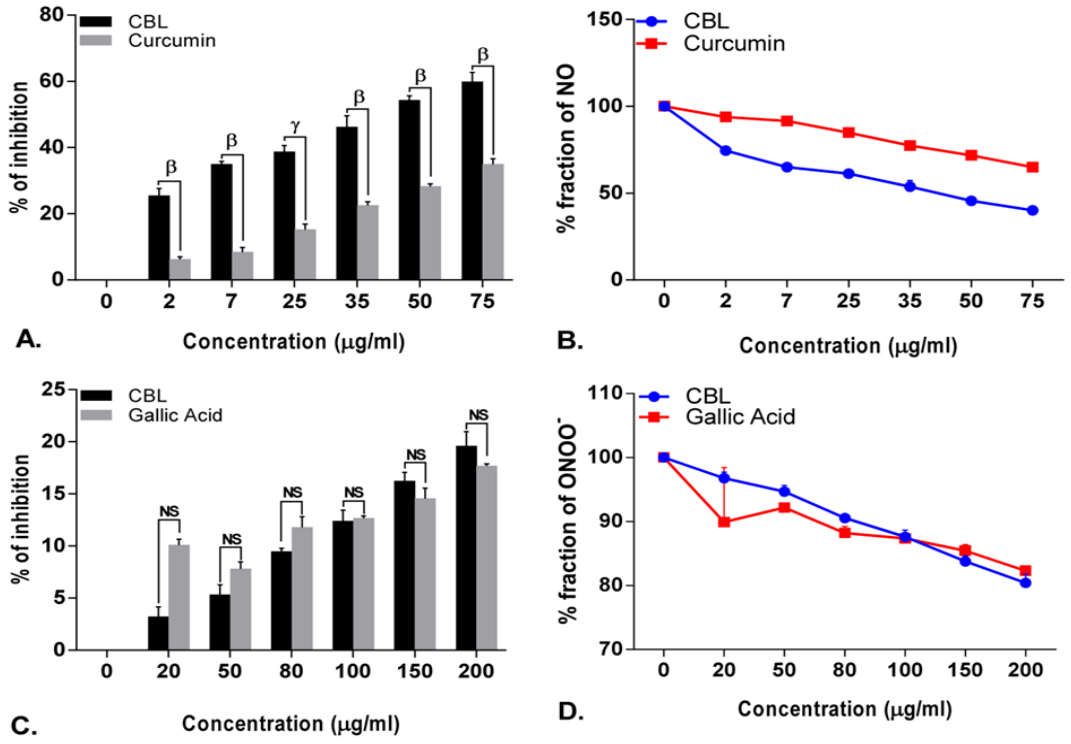


**Figure 32:** Antioxidant activity of *Croton bonplandianus*. **(A)** % inhibition of Nitric oxide (NO) Vs standard curcumin; **(B)** depicts unneutralized nitric oxide (NO). **(C)** % inhibition of Peroxynitrite ($OONO^-$) Vs standard gallic acid; **(D)** depicts unneutralized Peroxynitrite ($OONO^-$). Data expressed as mean ± S.D (n=6). α $p<0.05$; β $p<0.01$; γ $p<0.001$; NS-Non significant when compared with standard.

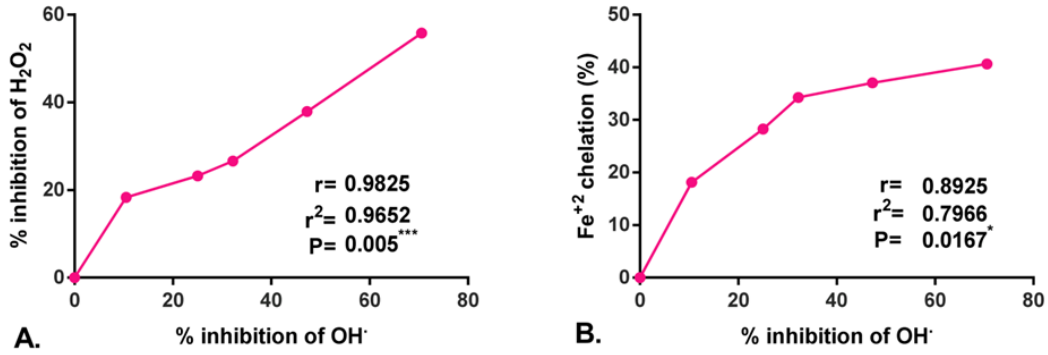


**Figure 33:** Pairwise correlation of $H_2O_2$ inhibition and $Fe^{2+}$-chelation Vs $OH^{\bullet}$ scavenging for *C. bonplandianus* represented in section **(A)** & **(B)**, respectively. All data are expressed as mean ± S.D. (n = 6). r= Pearson's correlation coefficient, $r^2$= coefficient of determination and *P*= significance value.

groups shown in Table 9. Final body weight was decreased only in $CCl_4$ groups (12.53 ± 1.39). On the other hand liver weight of $CCl_4$ group (5.16 ± 0.15) resulted in the highest relative liver weight (26.37 ± 1.40) among all the groups. Interestingly only high dose group (CBLH) prevented utmost percent of body weight changes. The relative liver weight of all the groups were closes another, except $CCl_4$ group.

**4.5.3. *In vitro* liver marker enzymes and biochemical parameters**

The effect of $CCl_4$ and the subsequent administration of silymarin and CBL on the various serum enzymatic and biochemical parameters are shown in Table 10. All the *in vivo* experimental parameters were increased in case of $CCl_4$ group and subsequently decreased with silymarin and CBL treatment except protein and albumin.

**4.5.6. Estimation of hepatic antioxidative enzymes: Catalase, Peroxidase, Superoxide dismutase and reduced glutathione**

Significant inhibition of enzymatic catalase and SOD (superoxide dismutase) and non-enzymatic reduced glutathione by CBL extract occurred in $CCl_4$ intoxicated mice when compared with the control (Figure 34). CBL treatment enabled significant increase in the percent of inhibition of catalase and reduced glutathione when compared with $CCl_4$ toxicated groups. On the other hand silymarin treatment significantly increase the percent of inhibition compared with the $CCl_4$ treated mice. On the other hand the activity of peroxidase enzyme in hepatic tissue is significantly lowered as a result of $CCl_4$ treatment (Figure 34). The peroxidase activity in the control group was 14.79 unit/mg tissues which were lowered 7.43 unit/mg tissues due to $CCl_4$ administration. The lowered peroxidase activity was

**Table 9:** Changes of body weight (g) and liver weight (g) in different experimental groups of hepatoprotective model. Data represented as mean ± SD of six observations.

| Group | Initial body weight | Final body weight | % body weight change | Liver weight | Relative liver weight |
|---|---|---|---|---|---|
| **Control** | 22.82 ± 0.65 | 25.84 ± 0.18 * | 11.69 ± 2.63 ▲ | 4.70 ± 0.16 | 18.21 ± 0.68 |
| **CCl4** | 22.06 ± 0.29 | 19.61 ± 0.50 ** | 12.53 ± 1.39 ▼ | 5.16 ± 0.15 NS | 26.37 ± 1.40 |
| **Silymarin** | 22.71 ± 0.54 | 24.67 ± 0.85 * | 7.92 ± 1.24 ▲ | 4.52 ± 0.21 NS | 18.33 ± 0.57 |
| **CBL (50 mg/kg BW)** | 23.22 ± 0.41 | 23.87 ± 0.17 * | 2.72 ± 1.08 ▲ | 5.07 ± 0.12 NS | 21.24 ± 0.42 |
| **CBL (100 mg/ kg BW)** | 22.05 ± 0.52 | 22.99 ± 0.48 ** | 4.06 ± 0.32 ▲ | 4.89 ± 0.25 NS | 20.88 ± 0.60 |
| **CBL (250 mg/ kg BW)** | 22.73 ± 0.76 | 24.59 ± 0.41 * | 7.57 ± 2.72 ▲ | 4.63 ± 0.22 NS | 18.83 ± 1.12 |

NS $p > 0.05$, *$p < 0.05$, **$p < 0.01$, ***$p < 0.001$. Final body weight was compared with initial body weight of corresponding group and liver weight of treated groups was compared with liver weight of control group. ▲ represents increase and ▼ represents decrease.

significantly elevated by CBLH (12.74 unit/mg tissue) when compared with the standard silymarin treated group (12.07 unit/mg tissue).

**4.5.7. *In vitro* liver marker enzymes and biochemical parameters**

The hepatoprotective potential of CBL extract was reflected through *in vitro* liver marker enzymes and biochemical parameters. The results were compared with the standard drug silymarin as shown in Table 11. The $CCl_4$ group showed the higher toxicity than the other groups.

**4.5.8. Lipid peroxidation (MDA level)**

Lipid peroxidation or MDA level in the treated groups are illustrated in (Figure 35). The MDA content was elevated from 8.99 µM/litre in control to 19.27 µM/litre in $CCl_4$ group. Significant results found when the elevated MDA level was lowered

**Table 10:** Describes the levels of various enzymatic and biochemical parameters in the serum of six (n=6) treated groups of hepatoprotective model. The data represented as mean ± SD of six observations.

| Parameters (units) | Control | $CCl_4$ | Silymarin | CBL (50 mg/kg BW) | CBL (100 mg/kg BW) | CBL (250 mg/kg BW) |
|---|---|---|---|---|---|---|
| **ACP (K.A.)** | 3.81 ± 0.04 | 13.13 ± 0.63$^{**}$ | 6.02 ± 0.48$^{*b}$ | 11.21 ± 0.23$^{***d}$ | 9.88 ± 0.73$^{**a}$ | 8.21 ± 0.22$^{**b}$ |
| **ALP (K.A.)** | 13.09 ± 0.30 | 31.16 ± 0.25$^{***}$ | 16.23 ± 0.35$^{***c}$ | 29.30 ± 0.48$^{***d}$ | 28.24 ± 0.35$^{***b}$ | 23.07 ± 0.66$^{***c}$ |
| **AST (u/ml)** | 63.34 ± 0.59 | 142.19 ± 0.66$^{***}$ | 82.66 ± 0.94$^{***c}$ | 141.70 ± 0.81$^{***d}$ | 127.72 ± 0.91$^{***b}$ | 108.49 ± 1.11$^{***c}$ |
| **ALT (u/ml)** | 47.94 ± 0.65 | 137.39 ± 0.61$^{***}$ | 56.53 ± 0.87$^{**c}$ | 123.18 ±0.39$^{***c}$ | 105.72 ± 1.11$^{***c}$ | 77.20 ± 0.32$^{***c}$ |
| **GGT (u/l)** | 3.76 ± 0.11 | 8.26 ± 0.52$^{**}$ | 4.90 ± 0.20$^{*b}$ | 7.06 ± 0.33$^{**d}$ | 6.32 ± 0.26$^{**d}$ | 5.60 ± 0.32$^{*b}$ |
| **Glucose (mg/dl)** | 57.04 ± 1.53 | 85.18 ± 1.19$^{**}$ | 63.85 ± 1.32$^{*b}$ | 81.72 ± 2.20$^{**d}$ | 72.15 ± 0.65$^{**c}$ | 67.41± 0.91$^{**b}$ |
| **Protein (g/dl)** | 5.93 ± 0.06 | 4.07 ± 0.05$^{***}$ | 5.72 ± 0.07$^{NSb}$ | 4.11 ± 0.06$^{***d}$ | 4.26 ± 0.09$^{***a}$ | 5.12 ± 0.31$^{*a}$ |
| **Albumin (g/dl)** | 4.54 ± 0.33 | 2.27 ± 0.20$^{*}$ | 3.43 ± 0.17$^{**a}$ | 2.52 ± 0.13$^{*d}$ | 2.87 ± 0.10$^{*d}$ | 3.03 ± 0.16$^{*d}$ |
| **Globulin (g/dl)** | 2.19 ± 0.02 | 0.84 ± 0.03$^{***}$ | 1.99 ± 0.03$^{*c}$ | 0.99 ± 0.03$^{***b}$ | 1.16 ± 0.03$^{***c}$ | 1.72 ± 0.04$^{**c}$ |
| **Bilirubin (mg/dl)** | 0.81 ± 0.04 | 2.04 ± 0.07$^{**}$ | 1.05 ± 0.05$^{**b}$ | 1.88 ± 0.09$^{**d}$ | 1.71 ± 0.04$^{**b}$ | 1.33 ± 0.04$^{**b}$ |
| **Urea (mg/dl)** | 35.43 ± 3.94 | 128.76 ± 6.38$^{**}$ | 58.16 ± 4.76$^{*b}$ | 116.46 ± 4.29$^{***d}$ | 100.51 ± 1.68$^{**b}$ | 78.24 ± 3.04$^{**b}$ |
| **Urea $N_2$ (mg/dl)** | 12.69 ± 0.96 | 72.55 ± 1.91$^{***}$ | 30.65 ± 0.91$^{***b}$ | 68.05 ± 1.38$^{***a}$ | 53.70 ± 1.45$^{***b}$ | 40.61 ± 1.24$^{**b}$ |
| **LDH (u/l)** | 240.73 ± 2.89 | 571.83 ± 4.41$^{***}$ | 296.01 ± 2.15$^{**c}$ | 548.55 ± 4.45$^{***c}$ | 502.66 ± 6.04$^{***b}$ | 340.50 ± 2.67$^{***c}$ |
| **Cholesterol (mg/dl)** | 68.66 ± 1.51 | 132.17 ± 2.38$^{***}$ | 90.37 ± 2.05$^{**c}$ | 113.38 ± 3.55$^{***b}$ | 101.35 ± 2.19$^{**b}$ | 93.22 ± 1.67$^{**b}$ |

$^{NS}$P= non significant (p> 0.05), $^{*}$P < 0.05, $^{**}$P < 0.01 and $^{***}$P < 0.001vs control group; whereas $^{d}$P= non significant (p> 0.05), $^{a}$P < 0.05, $^{b}$P < 0.01 and $^{c}$P < 0.001 vs $CCl_4$ group.

**Table 11:** Changes in the levels of various enzymatic and biochemical parameters of the culture supernatants of the experimental groups of hepatoprotective model. Data represented as mean ± SD of six observations.

| Parameters (units) | Control | $CCl_4$ | Silymarin | CBL (50 mg/kg BW) | CBL (100 mg/kg BW) | CBL (250 mg/kg BW) |
|---|---|---|---|---|---|---|
| **ACP (K.A.)** | 0.80 ± 0.04 | 1.95 ± 0.04$^{***}$ | 1.21 ± 0.03$^{**b}$ | 1.72 ± 0.03$^{***a}$ | 1.58 ± 0.04$^{**a}$ | 1.36 ± 0.05$^{**b}$ |
| **ALP (K.A.)** | 3.38 ± 0.05 | 8.06 ± 0.07$^{***}$ | 4.92 ± 0.23$^{**c}$ | 6.83 ± 0.14$^{***b}$ | 6.22 ± 0.12$^{**b}$ | 5.45 ± 0.23$^{**b}$ |
| **AST (u/ml)** | 15.54 ± 0.66 | 54.63 ± 0.75$^{***}$ | 20.32 ± 0.94$^{**c}$ | 43.98 ± 0.52$^{***d}$ | 40.30 ± 1.11$^{***b}$ | 28.52 ± 0.85$^{**b}$ |
| **ALT (u/ml)** | 7.71 ± 0.34 | 34.57 ± 1.64$^{**}$ | 13.95 ± 0.29$^{***b}$ | 29.29 ± 0.77$^{***d}$ | 26.28 ± 0.80$^{***a}$ | 18.42 ± 1.00$^{**c}$ |
| **GGT (u/l)** | 0.64 ± 0.03 | 1.16 ± 0.03$^{***}$ | 0.79 ± 0.04$^{*b}$ | 1.08 ± 0.03$^{***b}$ | 1.03 ± 0.01$^{***a}$ | 0.913 ± 0.02$^{***b}$ |
| **Bilirubin (mg/dl)** | 0.21 ± 0.02 | 0.67 ± 0.02$^{***}$ | 0.316 ± 0.02$^{**c}$ | 0.64 ± 0.03$^{***d}$ | 0.54 ± 0.02$^{***c}$ | 0.41 ± 0.02$^{**b}$ |
| **Protein (g/ dl)** | 7.49 ± 0.04 | 5.69 ± 0.27$^{**}$ | 7.05 ± 0.06$^{**a}$ | 5.99 ± 0.03$^{***d}$ | 6.63 ± 0.27$^{*a}$ | 6.91 ± 0.16$^{*b}$ |
| **LDH (u/l)** | 42.59 ± 1.10 | 211.01 ± 2.59$^{***}$ | 121.18 ± 1.36$^{***c}$ | 188.94 ± 2.78$^{***a}$ | 167.48 ± 3.04$^{***b}$ | 135.20 ± 1.49$^{***c}$ |

$^{NS}$P= non significant (p> 0.05), $^{*}$P < 0.05, $^{**}$P < 0.01 and $^{***}$P < 0.001vs control group; whereas $^{d}$P= non significant (p> 0.05), $^{a}$P < 0.05, $^{b}$P < 0.01 and $^{c}$P < 0.001 vs $CCl_4$ group.

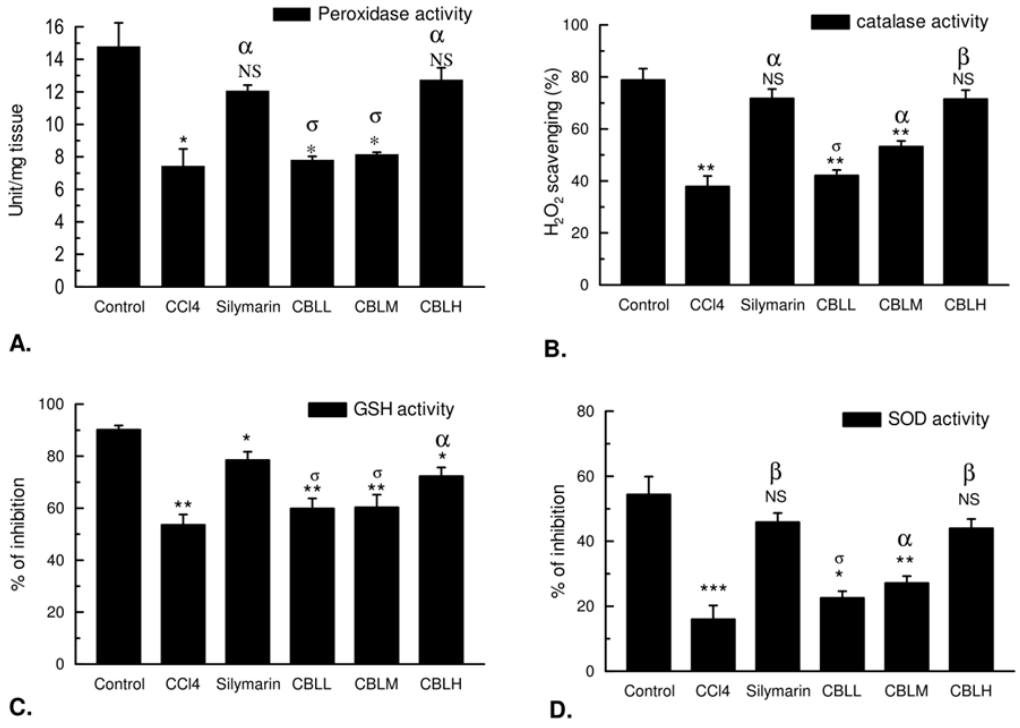


**Figure 34:** The effect of *Croton bonplandianus* on the **(A)** Peroxidase; **(B)** Catalase; **(C)** Reduced glutathione (GSH); **(D)** Superoxide dismutase (SOD) activities in $CCl_4$ intoxicated liver samples. Comparisons were made with control for statistical inference ('t' test for paired comparison) to interpret significant difference. Data expressed as mean ± S.D (n=6). $^{\alpha}$ p<0.05; $^{\beta}$ p<0.01; $^{\gamma}$ p<0.001; $^{NS}$-Non significant.

to 10.60 µM/litre after CBLH administration.

**4.5.9. MTT cytotoxic effect**

Viability of cells were decreased in the $CCl_4$ group significantly ($p<0.01$) compared to the control group (Figure 35). The viability of the cells in $CCl_4$ group was only (43.67 ± 6.11), where in the standard silymarin group the percent of viability of cells was (87.00 ± 5.29) which was very close to the control group. On the other hand, in the experimental groups, the cell viability was increased gradually. Percentage of cell viability in CBLH group (70.33 ± 8.02) was very close to the standard group.

**4.5.10. Measurement of the release of TNF- α**

Measurement of TNF-α release are demonstrated in the Figure 35. The level of TNF-α in control group was 120.32 ± 8.04 pg/ml, which was increased 1259.20 ± 96.96 pg/ml due to $CCl_4$ toxicity. However the TNF-α level decreased better by CBLH group (716.66 ± 73.06 pg/ml) when compared with the standard silymarin group (786.22 ± 49.70 pg/ml).

**4.5.11. Inhibition of nitric oxide (NO)**

$CCl_4$ toxicity resulted increases in NO release when compared to the control (Figure 35). However, significant ($p < 0.001$) lowering of NO level was observed in the treated groups. The NO level in silymarin and CBLH groups were 141.33 ± 12.70 and 175.33 ± 12.50 % respectively, when NO release of control was considered as 100 %.

**4.5.12. Detection of intracellular ROS generation**

Human hepato cell line WRL-68 was used to examine the effects of CBL under oxidative stress. $CCl_4$ increases oxidative stress levels in the liver tissue, and based on that study, it is speculated that $CCl_4$ may induce the oxidative stress in WRL-68 cells. Therefore, WRL-68 cells were treated with $CCl_4$ for 0–24 h, and intracellular oxidative levels were measured using the dichlorofluorescein assay. Figure 36 demonstrated that cells exposed to $CCl_4$ exhibited significantly increase in ROS levels. Tremendous decrease in fluorescence was detected at higher doses of CBL (200µg/ml) at 24h post exposure compared to the $CCl_4$ (Figure 36). The resulting change in fluorescence intensity gives strength to the hypothesis that CBL affects in the production of intracellular ROS.

**4.5.13.Histopathological examination**

There are several hiotological parameters showed the injury level of experimental groups as enlisted in Table 12. The haematoxilin-eosin staining of hepatocytes displayed clearly the well maintained hepatocellular integrity, healthy cellular architecture, and clear cytoplasm with prominent nucleus in the control group. But in the $CCl_4$ group, several damages have been observed. Hepatocytes of the $CCl_4$ groups showed hepatocellular

necrosis, bile duct proliferation, sinusoidal dialation, inflammation (leukocyte infiltration), vascular congestion, loss of structure of hepatic nodules, fatty

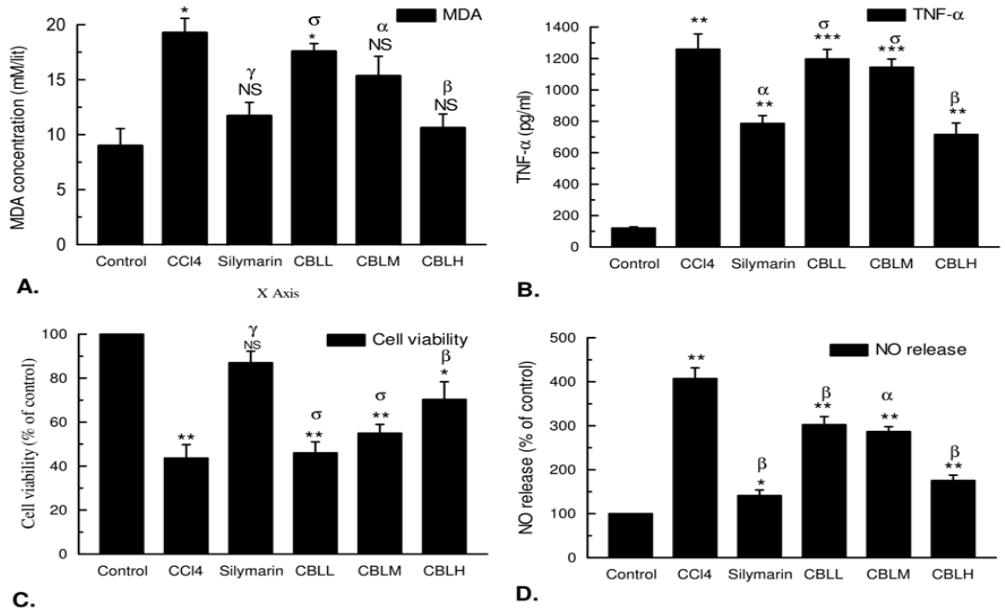


**Figure 35:** The effect of *Croton bonplandianus* on **(A)** MDA level; **(B)** TNF-α level; **(C)** Cell viability; **(D)** NO release activities in $CCl_4$ intoxicated liver samples. Comparisons were made with control for statistical inference ('t' test for paired comparison) to interpret significant difference. Data expressed as mean ± S.D (n=6). $^{\alpha}p<0.05$; $^{\beta}p<0.01$; $^{\gamma}p<0.001$; $^{NS}$-Non significant.

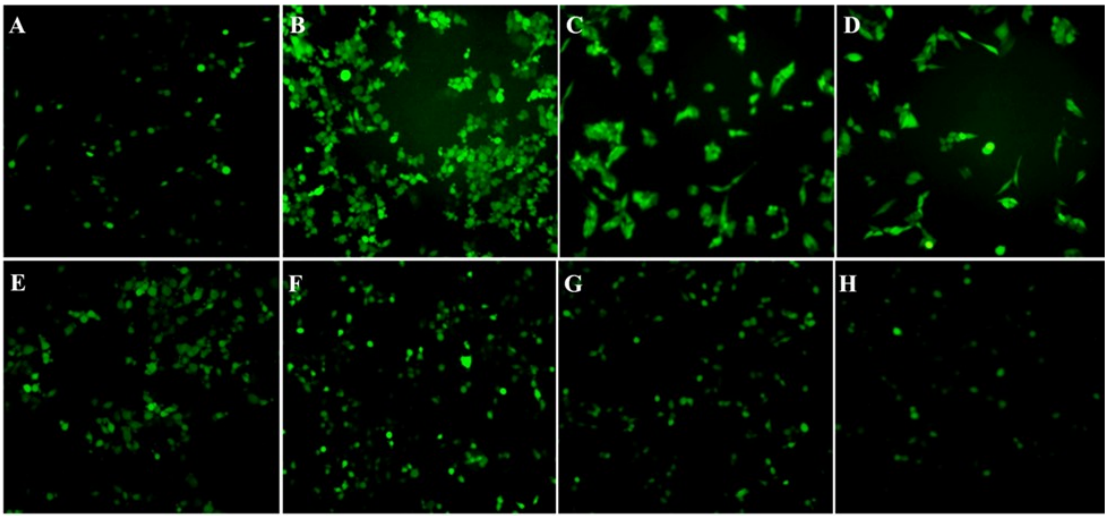


**Figure 36:** Effects of CBL in depletion of intracellular ROS production generated by $CCl_4$ in WRL-68 cells. Production of ROS was measured by cleavage of acetate group of non-fluorescent $H_2$DCFDA (2',7'-dichlorodihydrofluorescein diacetate) which convert into DCF (2′ ,7′ -dichlorofluorescein) highly fluorescent. Cells were exposed to $CCl_4$ before treatment with CBL 50, 80, 100, 150 and 200 µg/ml for 24 h. The ROS production displays the intensity of fluorescence through the images of WRL-68 cells treated with different concentration of CBL **(D-H)**, $CCl_4$ **(C)**, $H_2O_2$ **(B)** and control **(A)**.

infiltration, vascular degeneration and calcification. Most strikingly fibrosis, the thickening and scoring of connective tissue, as a result of injury was notified in the $CCl_4$ group (Figure 37, 38, 39). The injury level found in the $CCl_4$ group was down regulated by the administration of standard drug silymarin. Interestingly, in the present study it was observed that high dose of plant extract (CBLH) down regulates the injury better or similar compared to the standard silymarin.

**4.5.14. Molecular Docking**

The bioactive compounds of *Croton bonplandianus* was checked for possible interactions with several proteins playing the essential role in different metabolic pathways of humans and other major vertebrates. The proteins were chosen those have relationship with the health of the liver. These proteins acted as receptors required for molecular docking experiments. The ligands required to conduct the experiment are the compounds identified my GC-MS analysis of the plant extract. Upon a series of receptor-ligand interaction study, it was identified that each of the ligands has different binding affinity with the selected proteins. It is seen that α-amyrin has the highest interaction with all the receptors on an average followed by Campesterol and Ethyl iso-allocholate (Figure 40). On the other hand 1- Octacosanol has the least binding affinity with the receptors. For the comparative analysis a standard was used. Silymarin a proven drug against hepato toxicity was used as a standard in this regard. One of the phytochemical α-amyrin had a binding affinity better than silymarin with all the receptors on average. The highest binding affinity was found

**Table 12:** Describe the effect of CBL on liver histology parameters of the $CCl_4$ induced injured liver.

| Parameters studied | Control | $CCl_4$ | Silymarin | CBLL | CBLM | CBLH |
|---|---|---|---|---|---|---|
| **Hepatocellular necrosis** | 0 | 7 | 2 | 6 | 5 | 3 |
| **Bile duct prolifaration** | 0 | 2 | 0 | 2 | 1 | 1 |
| **Sinusoidal dilatation** | 0 | 1 | 0 | 1 | 0 | 0 |
| **Inflammation (leukocyte infiltration)** | 1 | 8 | 2 | 6 | 5 | 3 |
| **Vascular congestion** | 0 | 3 | 1 | 3 | 2 | 1 |
| **Loss of structure of hepatic nodules** | 0 | 5 | 2 | 4 | 2 | 2 |
| **Hepatocellular fibrosis** | 0 | 4 | 0 | 1 | 1 | 0 |
| **Fatty infiltration** | 0 | 1 | 0 | 0 | 0 | 0 |
| **Vacuolar degeneration** | 0 | 3 | 0 | 2 | 0 | 0 |
| **Calsification** | 0 | 2 | 1 | 1 | 1 | 0 |
| **Cumulative score** | 1 | 36 | 8 | 26 | 17 | 10 |

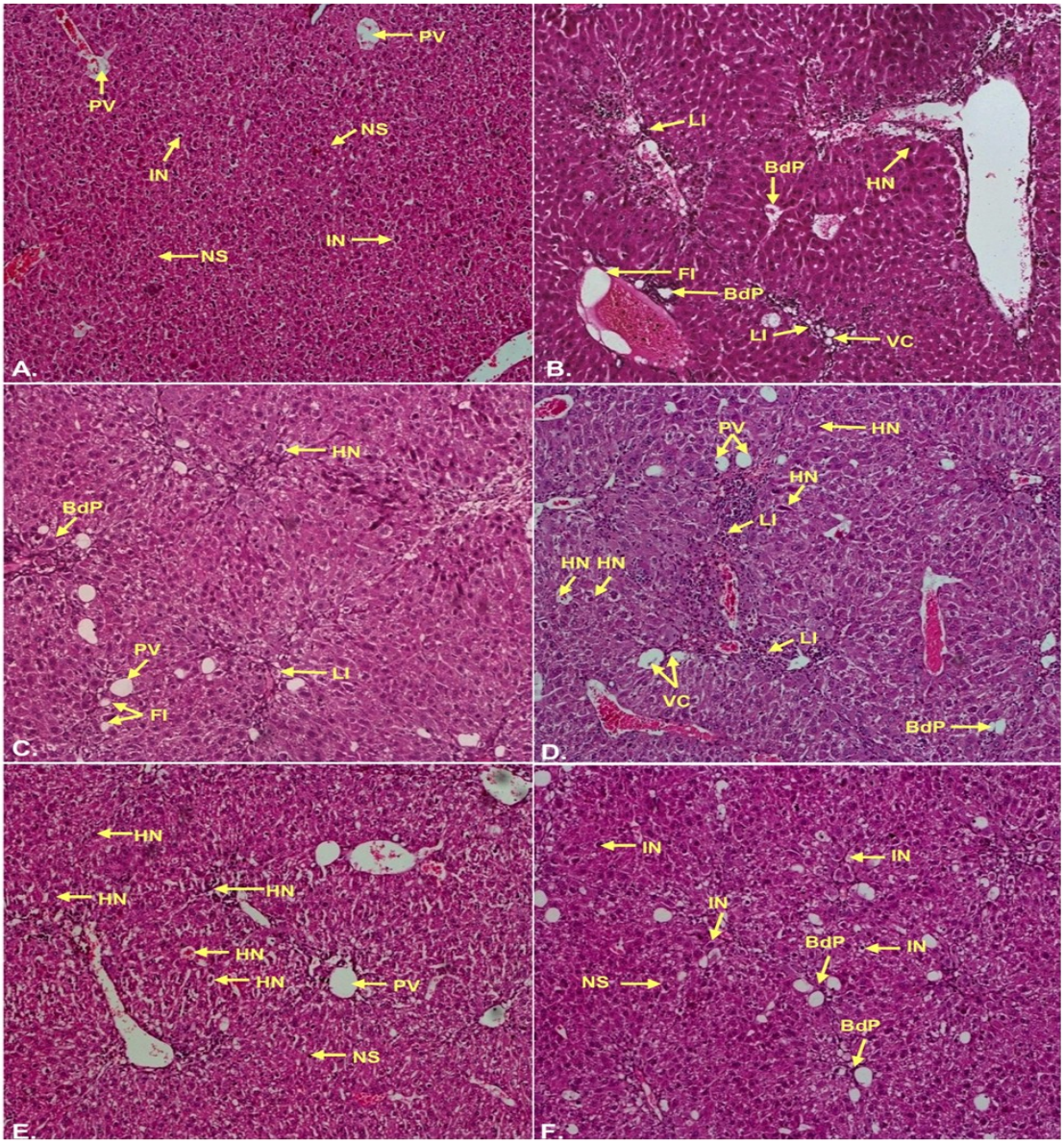


**Figure 37:** Photomicrographs (100×) of the histopathological examinations of the liver samples of different groups. Even though the extract treated groups possessed injury marks however, the extent of signs of injury were much lower in the extract treated groups compared to $CCl_4$ group. **(A)** Control group liver demonstrated normal liver architecture with normal sinusoids (NS), hepatocytes with intact nucleus (IN), un-inflamed portal vein (PV); **(B)** $CCl_4$ group liver demonstrated significant loss of hepatocellular architecture with extensive fatty infiltration (FI) leading to steatosis, bile duct proliferation (BdP), vascular congestion (VC) and haemorrhagic necrosis (HN) around portal vein. Loss of hepatic nodular structure and disorganized hepatocytes marked the $CCl_4$ induced liver damage; **(C)** Silymarin group demonstrated hepatoprotective activity by substantial amendment of proliferated bile duct (Bd) with normal sinusoids (NS) and intact portal veins (PV); **(D)** CBLL group was marked by less leukocyte infiltrations (LI), sinusoidal dilations (SD) and bile duct proliferation (BdP); **(E)** CBLM group reflected comparatively less haemorrhagic necrosis (HN) and fatty infiltrations (FI); **(F)** CBLH group demonstrated lowering of most of the injury signs however, leukocyte infiltrations (LI) could be identified in the liver samples.

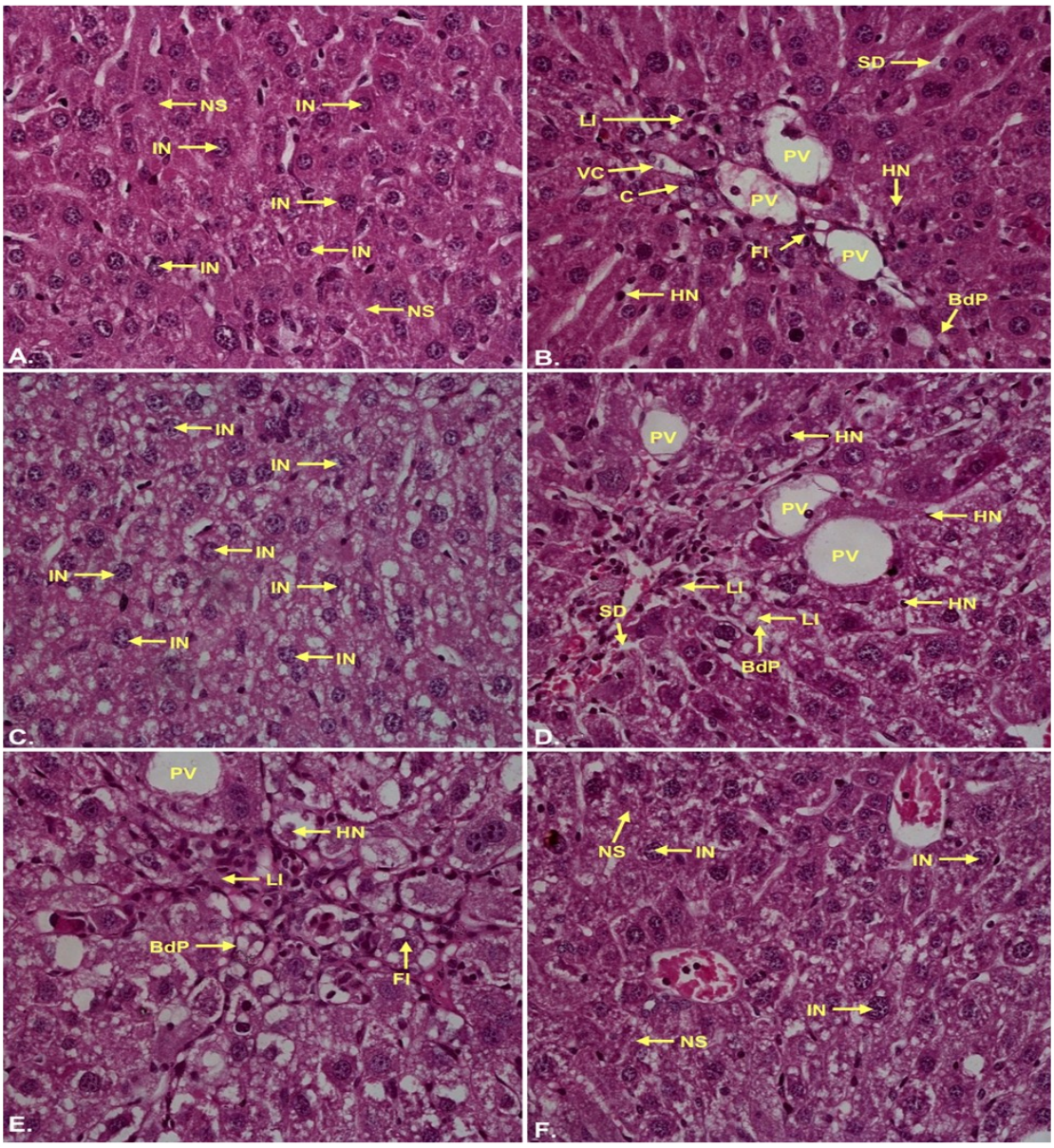


**Figure 38:** Photomicrographs (400×) of the histopathological examinations of the liver samples of different groups. **(A)** Control group liver sampled possessed well packed hepatocytes with intact nucleus (IN) and normal sinusoids (NS); **(B)** $CCl_4$ group liver possessed extensive fatty infiltrations (FI), Necrotic hepatocytes (N), prominent signs of inflammation with leukocyte infiltrations (LI), prominent calcification (C) around the congested vesicles (VC) with bile duct proliferations (BdP); **(C)** Silymarin group liver samples were characterized with normal sinusoids (NS) and intact nucleus (IN) containing healthy hepatocytes; **(D)** CBLL group demonstrated lower fatty infiltrations (FI), sinusoidal dilations (SD) and leukocyte infiltrations (LI); **(E)** CBLM group resulted in renewal of normal hepatic architecture with several hepatocytes with intact nucleus (IN) and lowered sinusoidal dilations (SD); **(F)** CBLH group showed near to normal hepatic architecture with predominantly intact nucleus (IN) containing normal hepatocytes and undiluted normal sinusoids (NS).

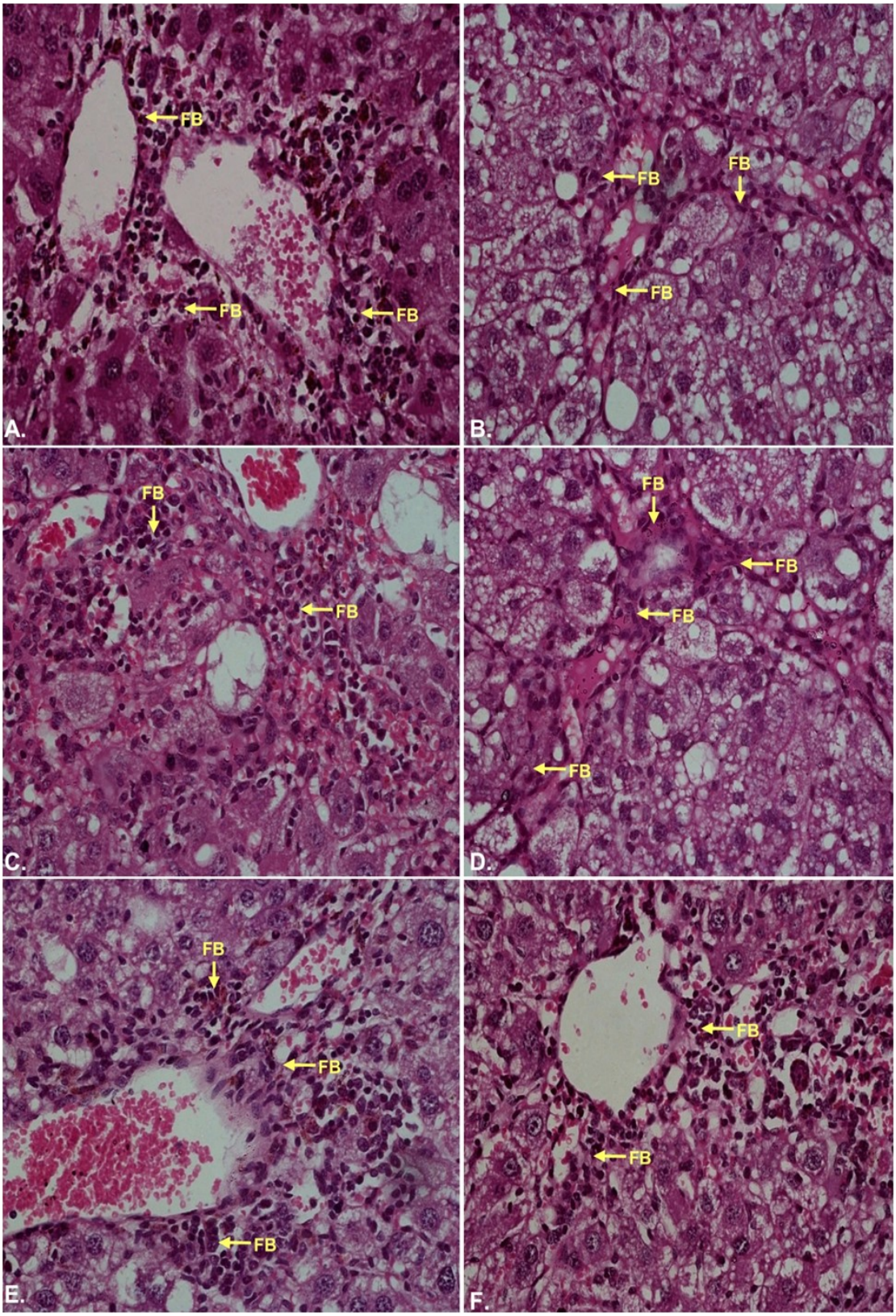


**Figure 39:** Photomicrographs (400×) of the histopathological examinations of the liver samples of $CCl_4$ group showing fibrosis.

between α-amyrin and a protein with PDB ID 3i7h which is the crystal structure of DDB1 in complex with H-Box Motif of HBX (Figure 41). NFκβ protein and Campesterol. also has good binding affinity and as seen in the molecular surface view of the protein moiety the ligand binds nicely inside a cavity in the protein surface (Figure 42).

## 4.6. Neuromodulatory activity

### 4.6.1. Acute toxicity study

CBL extract was administrated to the experimental animals up to 2,000 mg/kg body weight. However, at the 2000 mg/kg body weight dose, no sign of mortality and physiological deformation were observed in the experimental animals. Therefore, 50 mg/kg BW, 100 mg/kg BW and 250 mg/kg BW doses were selected as a low, medium and high dose in the *in vivo* neuromodulatory experiments.

### 4.6.2. Body and liver weight

Significant body weight changes were observed in $CCl_4$, CBLM and silymarin groups shown in Table 13. Final body

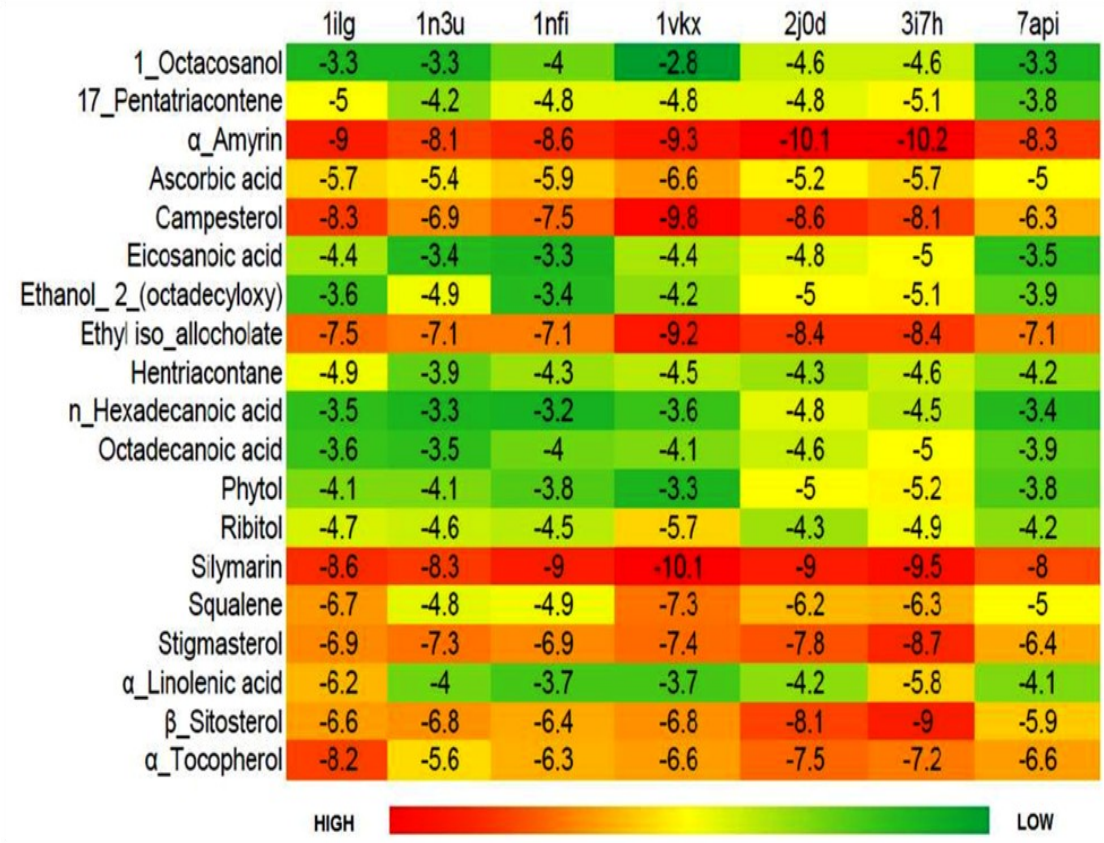


**Figure 40:** Heatmap based on binding energy among proteins and phytochemicals. The phytochemicals which served as ligands for molecular docking experiment are along the Y axis and the proteins are placed on the X-axis.

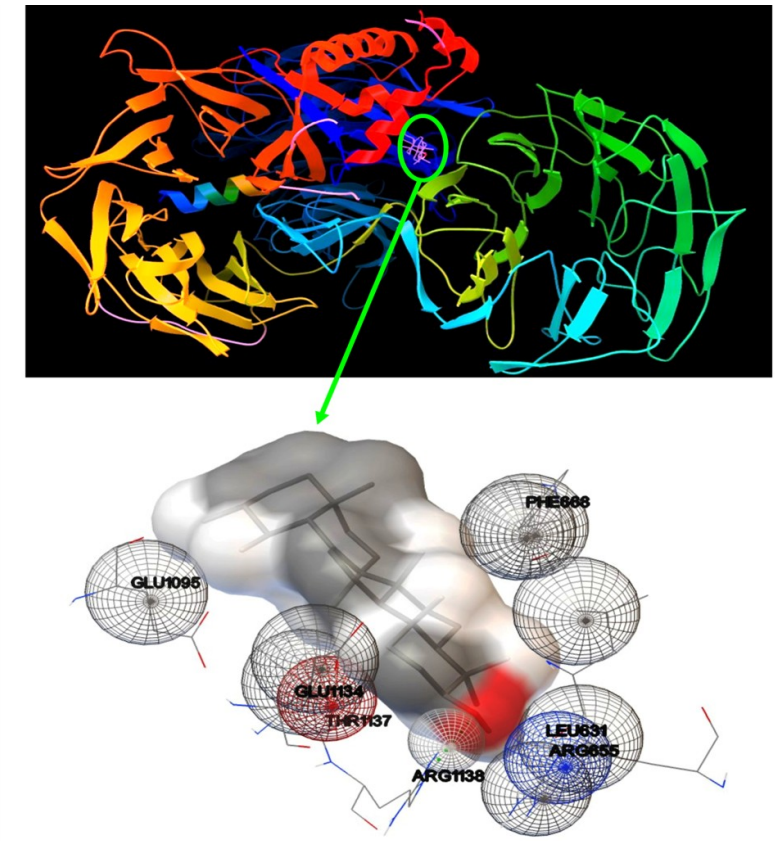


**Figure 41:** Molecular docking between Hepatitis BX protein and α-amyrin.

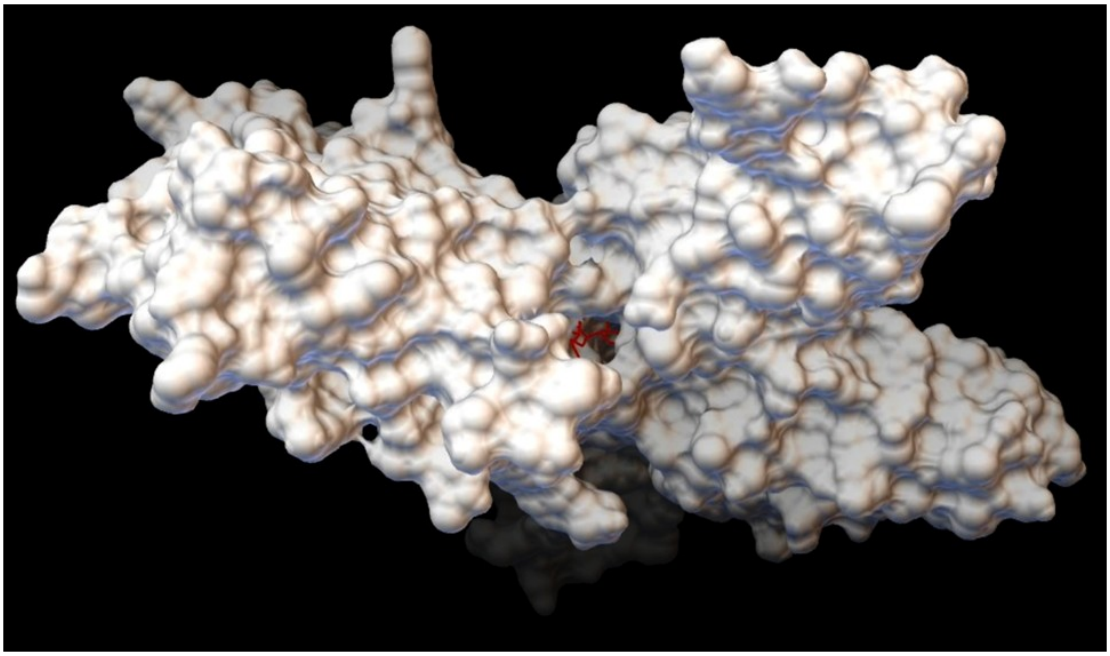

**Figure 42:** Molecular docking (molecular surface view) between NFκβ protein and Campesterol.

weight was decreased only in $CCl_4$ groups (12.53 ± 1.39). On the other hand liver weight of $CCl_4$ group (5.16 ± 0.15) resulted in the highest relative liver weight (26.37 ± 1.40) among all the groups. Interestingly only high dose group (CBLH) prevented utmost percent of body weight changes. The relative liver weight of all the groups were closes another, except $CCl_4$ group.

**4.6.3. Acetylcholinesterase (AChE) inhibitory activity**

The inhibition of cholinesterase enzyme activity is evident by fading of yellow color of the compound. In the present study, AChE inhibitory activity of CBLE was found to be 73.47±0.303% at 200 µg/ml with lower $IC_{50}$ value of 75.91±2.28 µg/ml. However, the $IC_{50}$ value of CBLE was found to relatively higher than standard serine (0.02±0.005 µg/ml).

**4.6.4. Effects of CBLE on scopolamine-induced memory impairment in mice**

Table 14 revealed that the initial latency time to enter the dark chamber was significantly longer in the mice given only scopolamine as compared to the control group suggesting amnesic effect of mice. The treatment with CBLE significantly ($P \leq 0.001$) attenuated the scopolamine induced memory deficit in mice to a great extent and also associated with the short-term memory (STL) improvement suggesting anti-amnesic effect of extracts in the scopolamine induced rodent model. While considering brain AChE-inhibitory activity, CBLE was also recorded to be reversed the scopolamine induced memory impairment in mice by increasing cholinergic activity through the inhibition of AChE (Figure 43 A).

**4.6.5. Estimation of hepatic antioxidative enzymes: DPPH, Catalase, Superoxide dismutase and reduced glutathione**

Significant inhibition of enzymatic catalase and SOD (superoxide dismutase) and non-enzymatic reduced glutathione by CBL extract occurred in scopolamine induced mice when compared with the control and positive control donepezil (Figure 43, 44, 45). CBL treatment

**Table 13:** Changes of body weight (g) and liver weight (g) in different experimental groups of neuromodulation. Data represented as mean ± SD of six observations.

| Group | Initial body weight | Final body weight | % body weight change |
|---|---|---|---|
| **Control** | 34.01±1.61 | 35.99±0.71 | 5.51±3.06▲ |
| **Scopolamine** | 34.19±1.44$^{NS}$ | 29.71±0.81$^{*}$ | 13.03±3.13▼ |
| **Donepezil** | 35.17±1.79$^{NS}$ | 36.66±1.72$^{NS}$ | 4.04±2.24▲ |
| **CBL (50 mg/kg BW)** | 33.74±1.42$^{NS}$ | 35.36±0.88$^{NS}$ | 4.57±2.85▲ |
| **CBL (100 mg/kg BW)** | 33.48±2.22$^{NS}$ | 35.34±0.8$^{NS}$ | 5.34±4.13▲ |
| **CBL (250 mg/kg BW)** | 32.34±1.00$^{NS}$ | 35.42±0.98$^{NS}$ | 8.65±3.45▲ |

NS $p > 0.05$, *$p < 0.05$, **$p < 0.01$, ***$p < 0.001$. Final body weight was compared with initial body weight of corresponding group and liver weight of treated groups was compared with liver weight of control group. ▲ represents increase and ▼ represents decrease.

**Table 14:** Effect of CBLE on scopolamine induced memory impairment in the passive avoidance test.

| Groups | IL (Sec.) | STL (Sec.) |
|---|---|---|
| **Group I (Control)** | 26.31 ± 3.57 | 149.65 ± 3.76 |
| **Group II (SCP)** | 106.35 ± 6.99$^{***}$ | 83.97 ± 4.99$^{**}$ |
| **Group III (SCP + Donepezil)** | 40.50 ± 4.29$^{NS\ \beta}$ | 178.46 ± 5.26$^{**\ \beta}$ |
| **Group IV (SCP + CBL-50 mg/kg BW)** | 91.35 ± 3.61$^{***\ \alpha\ B}$ | 135.81 ± 4.10$^{NS\ \gamma\ A}$ |
| **Group V (SCP + CBL-100 mg/kg BW)** | 71.52 ± 5.07$^{*\ \alpha\ B}$ | 146.25 ± 3.66$^{NS\ \gamma\ A}$ |
| **Group VI (SCP + CBL-250 mg/kg BW)** | 58.61 ± 3.05$^{**\ \alpha\ B}$ | 160.29 ± 4.58$^{NS\ \gamma\ D}$ |

IL – Initial latency; STL – Step through latency; SCP - Scopolamine; * p≤0.05; ** p≤0.01; *** p≤0.001; NS = Non significant Vs Control group; α p≤0.05; β p≤0.01; γ p≤0.001; δ = Non significant Vs Scopolamine induced group; A p≤0.05; B p≤0.01; C p≤0.001; D = Non significant Vs SCP + Donepezil group. Data represented as mean ± SD.

enabled significant increase in the percent of inhibition of catalase and reduced glutathione when compared with scopolamine induced group. On the other hand, donepezil treatment significantly increase the percent of inhibition compared with the scopolamine treated mice. On the other hand the inhibition of DPPH in brain tissue is significantly lowered as a result of scopolamine treatment (Figure 43B). The inhibition of DPPH activity significantly higher when the scopolamine induced mice simultaneously treated with standard drug donepezil and different doses of CBL extract.

**4.6.6. Lipid peroxidation (MDA level)**

Lipid peroxidation or MDA level in the treated groups are illustrated in (Figure 44 B). Significant results found when the elevated MDA level was lowered after CBLH administration.

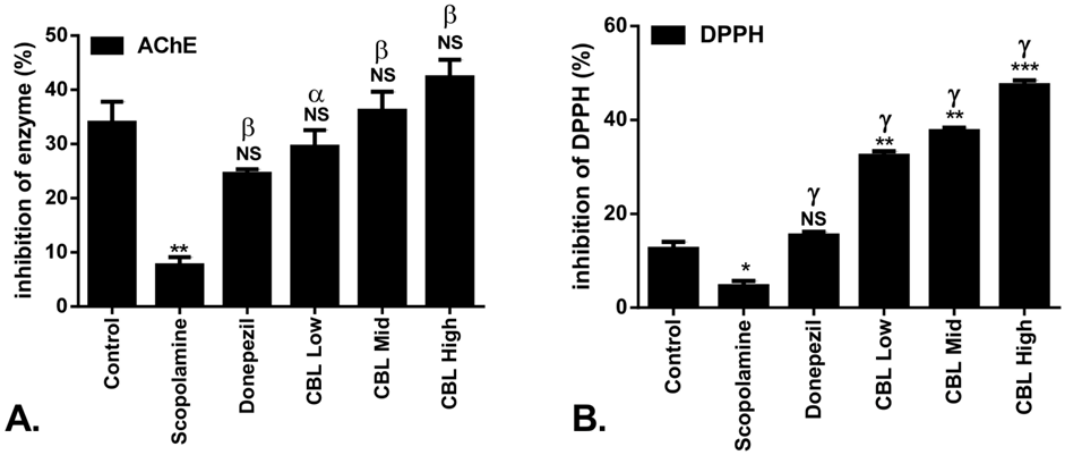


**Figure 43:** Effect of CBLE on scopolamine induced memory impairment in mice. **A.** AChE, **B.** DPPH activity of CBLE extract. * p≤0.05; ** p≤0.01; *** p≤0.001; NS = Non significant Vs Control group; $^{\alpha}$ p≤0.05; $^{\beta}$ p≤0.01; $^{\gamma}$ p≤0.001; $^{\delta}$ = Non significant Vs Scopolamine induced group. Data represented as mean ± SD.

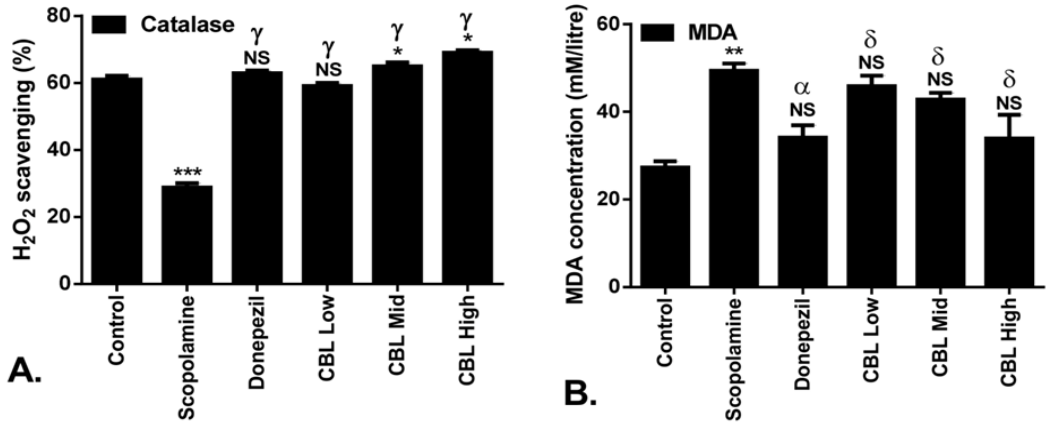


**Figure 44:** Effect of CBLE on scopolamine induced memory impairment in mice. **A.** Catalase, **B.** MDA (Lipid peroxidation) activity of CBLE extract. * p≤0.05; ** p≤0.01; *** p≤0.001; NS = Non significant Vs Control group; $^{\alpha}$ p≤0.05; $^{\beta}$ p≤0.01; $^{\gamma}$ p≤0.001; $^{\delta}$ = Non significant Vs Scopolamine induced group. Data represented as mean ± SD.

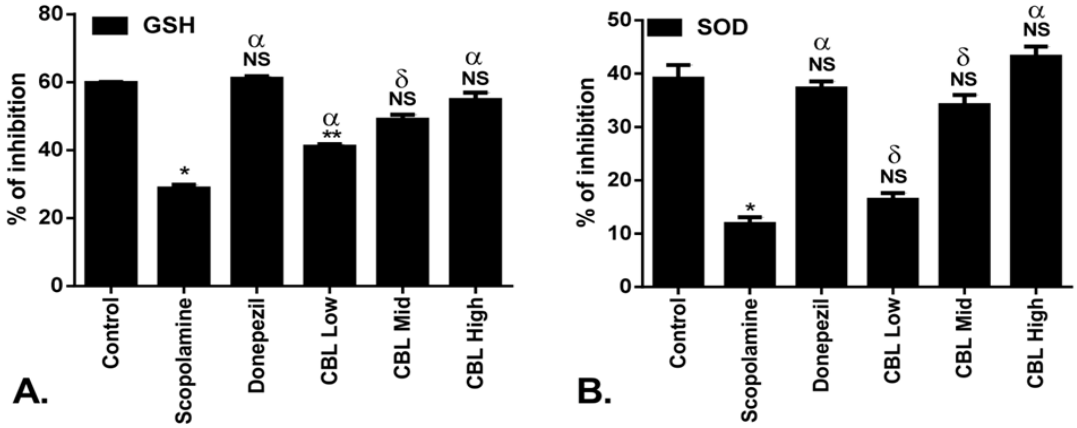


**Figure 45:** Effect of CBLE on scopolamine induced memory impairment in mice. **A.** GSH, **B.** SOD (Superoxide dismutase) activity of CBLE extract. * p≤0.05; ** p≤0.01; *** p≤0.001; NS = Non significant Vs Control group; $^{\alpha}$ p≤0.05; $^{\beta}$ p≤0.01; $^{\gamma}$ p≤0.001; $^{\delta}$ = Non significant Vs Scopolamine induced group. Data represented as mean ± SD.

**4.5.13.Histopathological examination**

There are several hiotological parameters showed the injury level of experimental groups. The haematoxilin-eosin staining of mice brain showing severe chromatolysis (arrows), Gliosis and edema in cortex. CBL extract (250mg/kg BW) showed moderate necrotic and degenerative changes. On the other hand in Hippocampus region control mice showed a normal glial cell layer, molecular layer and Purkinje layer. Scopolamine induced mice brain showed severe chromatolysis of nuclear material and most of the Purkinje neurons are necrotic. CBL extract (250mg/kg BW) showed significantly less necrotic degeneration of Purkinje neurons, lysis of glial cells.

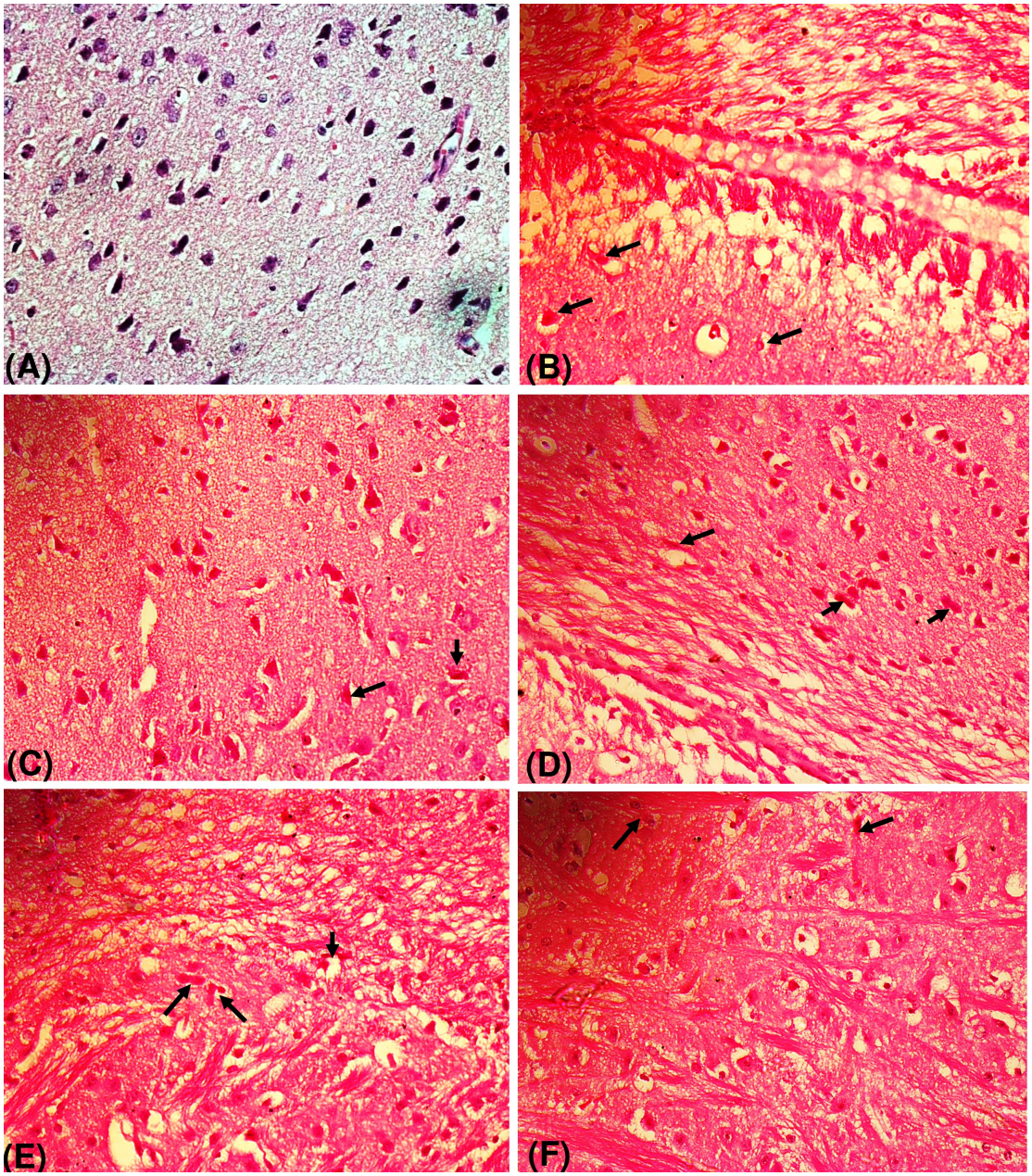


**Figure 46:** Photomicrograph control and treated mice brain (cortex, A-F), 40X. **(A)** Control mice showing various types of normal neurons, glial cells arranged in several layers. **(B)** Scopolamin induced mice brain showing severe chromatolysis (arrows), Gliosis and edema in cortex. **(C)** Mice brain exposed to donepzile showing less necrotic (arrows) and degenerative changes with normal neurons and glial cells. **(D)** CBL extract (50mg/kg BW) showing marked gliosis (arrows) and reduced severity of necrotic and degenerative lesions in brain cortex compared to B. **(E)** CBL extract (100mg/kg BW) showing marked gliosis (arrows) and reduced severity of necrotic and degenerative lesions in brain cortex compared to B and D. **(F)** CBL extract (250mg/kg BW) showing moderate necrotic and degenerative changes compared to B, D and E.

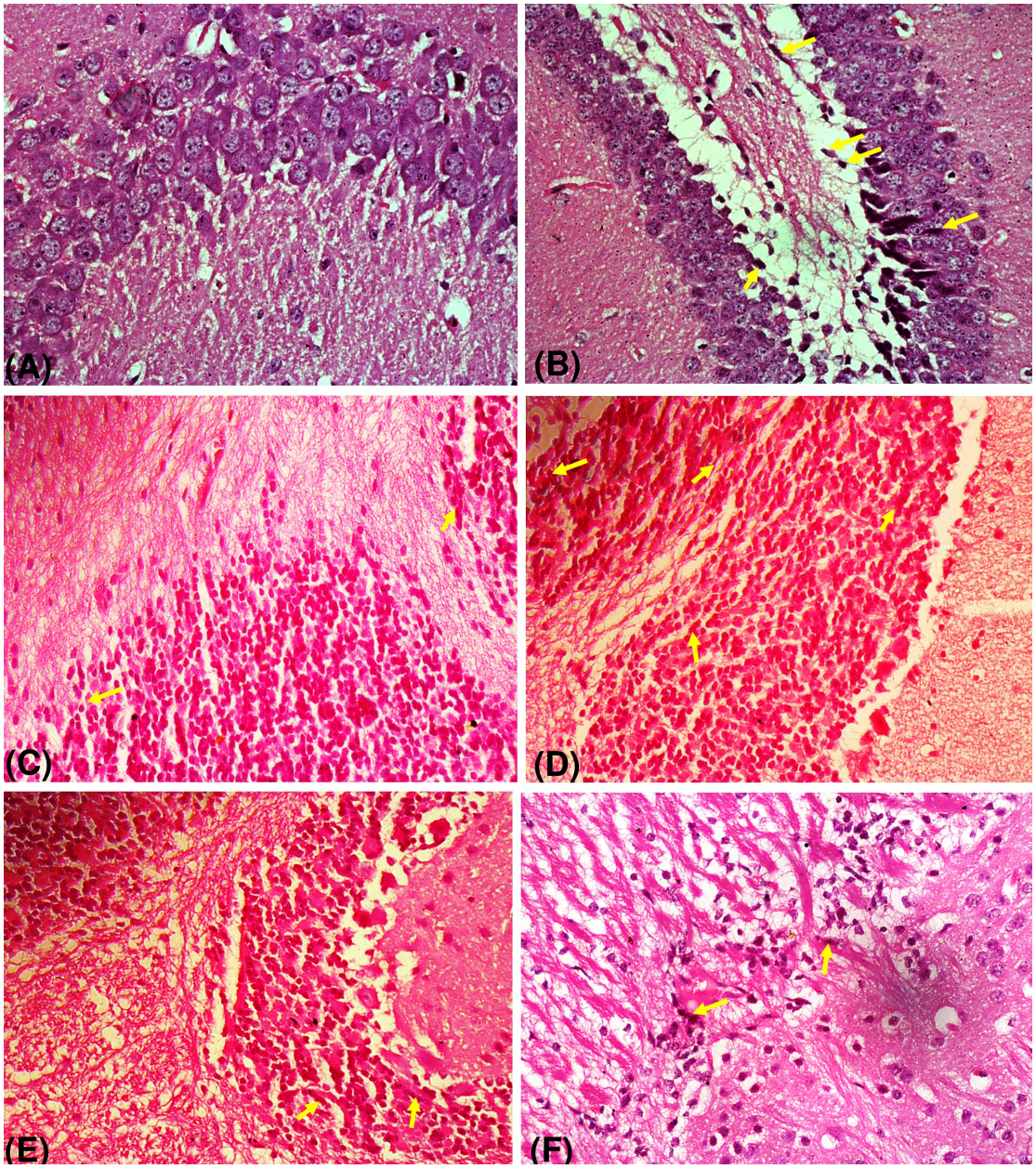


**Figure 47:** Photomicrograph control and treated mice brain (Hippocampus region, A-F), 40X. **(A)** Control mice showing a normal glial cell layer, molecular layer and Purkinje layer. **(B)** Scopolamine induced mice brain showing severe chromatolysis of nuclear material (arrows) and most of the Purkinje neurons are necrotic. **(C)** Donepzil exposed mice showing reduced severity of necrotic (arrows) and degenerative lesions in hippocampus of the brain. **(D)** CBL extracts (50mg/kg BW) showing necrotic degeneration of Purkinje neurons, lysis of glial cells (arrows) compared with B. **(E)** CBL extracts (100mg/kg BW) showing moderate necrotic degeneration of Purkinje neurons, lysis of glial cells (arrows) compared with B and D. (**F)** CBL extract (250mg/kg BW) showing significantly less necrotic degeneration of Purkinje neurons, lysis of glial cells (arrows) compared with B, D and E.